2022

Development of Gene Regulatory Elements for Biosensing Applications

Mallory N. Bates
Wright State University

DEVELOPMENT OF GENE REGULATORY ELEMENTS FOR BIOSENSING

APPLICATIONS

A Thesis submitted in partial fulfillment of the

requirements for the degree of

Master of Science in Biomedical Engineering

by

MALLORY N. BATES

B.S.B.E, Wright State University, 2020

2022

Wright State University

WRIGHT STATE UNIVERSITY
GRADUATE SCHOOL

4/20/2022

I HEREBY RECOMMEND THAT THE THESIS PREPARED UNDER MY
SUPERVISION BY Mallory N. Bates ENTITLED Development of Gene Regulatory
Elements for Biosensing Applications BE ACCEPTED IN PARTIAL FULFILLMENT
OF THE REQUIREMENTS FOR THE DEGREE OF Master of Science in Biomedical
Engineering.

_____

Tarun Goswami, D.Sc.
Thesis Director

_____

Subhashini Ganapathy, Ph.D.
Chair, Biomedical, Industrial &
Human Factors Engineering

Committee on Final Examination:

_____
Jaime E Ramirez-Vick, Ph.D.

_____
Ulas Sunar, Ph.D.

_____
Tarun Goswami, D. Sc.

_____
Barry Milligan, Ph.D.
Vice Provost for Academic Affairs
Dean of the Graduate School

ABSTRACT

Bates, Mallory, N. M.S.B.M.E., Department of Biomedical, Industrial, and Human Factors Engineering, Wright State University, 2022. Development of Gene Regulatory Elements for Biosensing Applications

21% of U.S adults experienced mental illnesses in 2020. Nearly 1 in 4 active- duty military personnel showed signs of mental health conditions in 2014 [89]. Mental health can be identified in the body by different biomarkers. These biomarkers potentially could be controlled by riboswitches, which could help mental illnesses and regulate diseases. Riboswitches are desirable in these cases due to responding without affecting vital functions. Riboswitches are located in mRNA and switch "ON" or "OFF" depending on the concentration of a biomarker [13]. In this research, riboswitches were re-engineered to take a known riboswitch and control its response in the presence of a biomarker. This was done by computationally changing $PreQ_1$, a known riboswitch that has the smallest aptamer, and then experimentally testing against biomarkers, dehydroepiandrosterone-sulfate (DHEA-S), Serotonin, Cortisol, Dopamine, Epinephrine, and Norepinephrine.

A total of 7 variant riboswitches were tested in this research, 4 created computationally and 3 created in research [53]. The results from these variants showed that variants 1 and 2 had different responses to DHEA-S then the expected $PreQ_1$ response. A dose response test confirmed this by having a downward trend as DHEA-S concentration increased. In conclusion of this research, riboswitches can be re-engineered to have a different response to biomarkers but keep the same structure.

TABLE OF CONTENTS

LIST OF FIGURES

LIST OF TABLES

ACKNOWLEDGMENTS

1. **Introduction**

  The body has self-made processes to help regulate different levels of proteins, analytes, and many other cellular metabolites. This prevents systems from deteriorating and helps keep homeostasis throughout the body. An example of this system in action would be if there was a high of serotonin in the body. A biomarker would recognize this surplus and transmit data to all systems that can regulate serotonin. The regulation part of this system would tell the body to stop producing serotonin and in addition have the body reduce the surplus as well.

  In the above example, riboswitches would help regulate the serotonin through RNA. An analyte or biomarker would bind to the aptamer of the riboswitch. The riboswitch would respond through producing proteins or stopping the production. Depending on the purpose of the riboswitch, proteins that would be produced would help decrease the surplus serotonin. If the riboswitch stops producing proteins, then the riboswitches' purpose would be to help production of serotonin.

  Riboswitches are RNA-based biological sensing elements that bind with metabolites without the need for protein involvement [58, 79]. They are used to regulate levels of biomarkers through the expression of proteins [61]. There are 17 different types of riboswitches that have been discovered and more than 100 are continuing to be experimentally validated [61]. Synthetic riboswitches are being engineered to help with gene therapy [8].

Biomarkers are cellular, biochemical, or molecular alterations measured in biological media, such as human tissues, cells, or fluids [19]. These markers have been studied as potential medical signs leading to disease. Biomarkers can be used to explain changes in the body that lead to mental illnesses, cardiovascular disease, and specific types of cancer [4]. Riboswitches can be used to regulate biomarkers. Identifying riboswitch and biomarker connections will lead to the regulation of these biomarkers [3]. In this research, different biomarkers will be tested against one riboswitch. After manipulating the riboswitch, the biomarkers response will be recorded.

PreQ$_1$ is the riboswitch used in this research. It was chosen due to having the smallest known aptamer with 34 nucleotides [23]. The biomarkers examined in this research are dehydroepiandrosterone-sulfate (DHEA-S), Serotonin, Cortisol, Dopamine, Epinephrine, and Norepinephrine. The biomarkers are shown in Table 1 along with related health conditions they influence.

Biomarker	Related health condition(s)
DHEA-S	Cognitive function [26]
Serotonin	Mood regulation, appetite, antidepressant [69]
Cortisol	Stress hormone, acute stress, low-blood glucose, obesity, depression, diabetes [47,69]
Dopamine	Feelings of happiness [69]
Epinephrine	Drives automatic nervous system emergency response, increases heart rate, blood pressure [69]
Norepinephrine	Stress hormone, high glucose, increased heart rate, anxiety, high blood pressure [69]

Table 1: Biomarkers and their related health conditions

Synthetic riboswitches could be extended to work with biomarkers to help with mental illnesses and regulate diseases. In 2020, twenty one percent of U.S adults experienced mental illnesses (52.9 million people). People with depression have a 40% higher risk of developing cardiovascular and metabolic diseases [89]. Nearly 1 in 4 active-duty military personal showed signs of a mental health condition in 2014 [89]. Using riboswitches as a potential way to solve problems is desirable because they can respond without affecting vital functions. Each riboswitch has different variants that respond in the same manner. A synthetic riboswitch would have the same design in the RNA makeup but would respond inversely. This can be done through the aptamer section of the riboswitch [81].

1.1 Motivation

The motivation behind this project was to engineer a variant riboswitch that has the structure of $PreQ_1$ but acts the reverse in the presence of biomarkers. This would show that it is possible to create a synthetic riboswitch from a known structure to change the outcome of proteins. From previous research, an approach that combines computational software and experimental data has shown to create such riboswitch. $PreQ_1$ is known to have a small aptamer with less nucleotides compared to other riboswitches [26,69].

In addition to a small aptamer, $PreQ_1$ has an ideal structure of the aptamer, which will be helpful when creating different designs in software. $PreQ_1$ has also been researched with the purpose of creating synthetic designs [72]. This research will be

referred to, as well as variants already created [53]. Known and newly created variants will be tested with the same biomarkers to compare as well.

The tests that will be used in this research are known procedures. This will help eliminate multiple variables needed to be modified and keep the focus of this research on the design and success of the variant riboswitches.

2. Literature Review

2.1 Riboswitches

A riboswitch is made of two parts; an aptamer and expression platform, located within the mRNA [15]. A riboswitch operates when a metabolite abundance meets a threshold, the ligand binds to the aptamer [60]. This leads to a downstream affect by the expression platform with a conformational change [2]. The conformational change generates the expression platform to either be in an "ON" or "OFF" state [61]. Aptamers bind to ligands with affinities and selectivity [6]. The complexity of the aptamer and ligand separately make it challenging to engineer [5]. Every riboswitch will be reengineered differently based on the chemical composition of that specific riboswitch [62]. Although a significant amount of research has been done, due to the specific methods needed, most aptamers have not been converted to functional riboswitches [56]. "Existing approaches rely on qualitative design by experts, combinational library generation and high-throughput screening, which have limited the breadth of riboswitch-based applications [12]." There is no way to predict ligand specificity through aptamer sequences [24].

Riboswitches have a wide range of classes with representatives within. Ronald R Breaker has distributed these classes and ligands [51, 71]. There are coenzymes, amino acids, signaling molecules, ions, nucleotide derivatives, and other metabolites [52]. Riboswitches are mostly found in bacteria [7]. "In the case of Bacillus subtilis, more than 4% of genes are predicted to be under the regulation of riboswitches and assorted cis-

regulatory elements" [24]. In 2012, Breaker stated there was currently 17 experimentally

validated riboswitch classes and potentially more than 100 classes still awaiting

discovery [32, 61]. Each riboswitch class can have multiple representatives, for example

the TPP riboswitch has more than 15,000 representatives that are known [36, 39]. The

structure of each riboswitch is made up of different nucleotides: adenine, uracil, cytosine,

and guanine [44]. The bonding of these nucleotides' forms knotting and folding of the

riboswitch [54].

Riboswitches can be placed into two large groups: pseudoknotted and junctional

riboswitches [45]. A pseudoknotted riboswitch is "predominantly on the basis of a single

pseudoknot, a knot-shaped conformation formed through base pairing between a loop of

an RNA stem-loop structure and an outside region" [82]. "Junctional riboswitches

contain a multi-helical junction which connects various numbers of helices" [82]. Other

than psuedoknots and junction loops; hairpins, stem loops, and kissing loops are also

structural elements. These can also play a part in different bonding [73].

Bonding in riboswitches is one controlling factor for ligand affinity [67].

Hydrogen bonding is most important for specificity of recognition to the ligand [83].

Ligands have donors and acceptors for hydrogen bonding [76]. When reengineering

riboswitches, changing a nucleotide can change the geometric shape and leads to the

recognition of the ligand [35, 40]. Hydrogen bonding is a dipole-dipole attraction

between molecules. This attraction comes from a hydrogen molecule and an

electronegative molecule such as oxygen, nitrogen, or fluorine [43]. For RNA, the

nitrogen bases are helping to form temporary hydrogen bonds [82].

In Figure 1, riboswitch diversity is shown. This image also shows the mechanisms

of gene control in bacteria. The portion that will be used in this research is in the section

A of the image. The figure shows how the aptamer encounters the ligand and from there

responses are shown. The response is based on the riboswitch. The aptamer and ligands

affinity and sizes determine if they would come into contact [1].
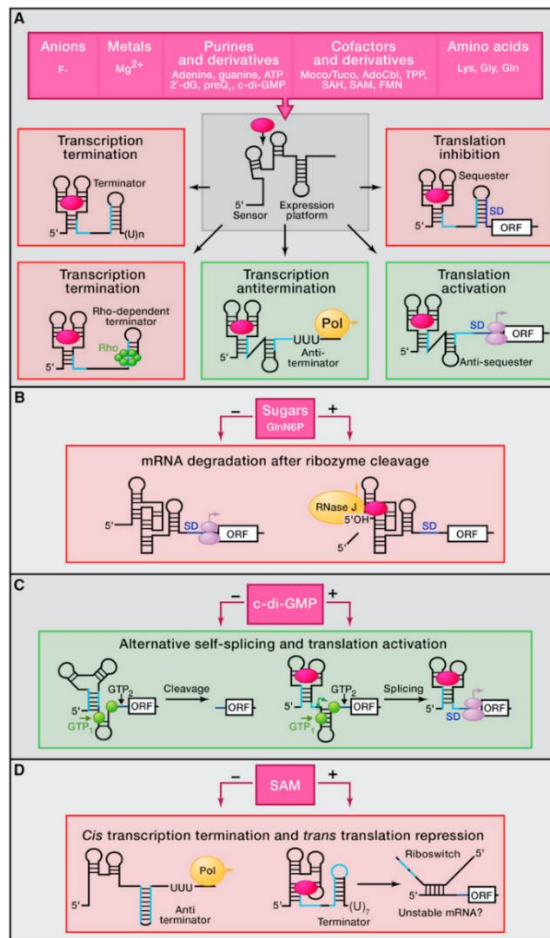
Figure 1. Diversity of riboswitches [2]

2.2 PreQ$_1$

PreQ$_1$ is known from its interaction to produce the hypermodified guanine

nucleotide, queuosine (Q). This is a multistep reaction that starts with GTP then going to

PreQ$_0$ and PreQ$_1$ to end in Q, as shown in Figure 2.
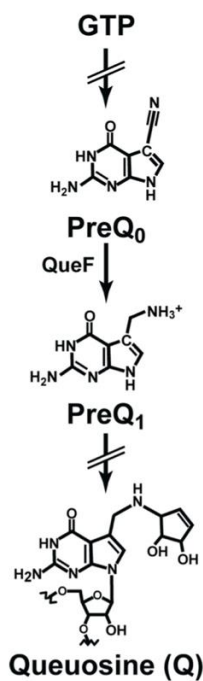
Figure 2. Schematic diagram of queuosine-precursor and preQ$_1$ riboswitch organization
[23]

There are two different subclasses of PreQ$_1$ based on where they are found, type I and II.

Type I is found in *T. tengcongensis* and type II in *Bacillus subtilis* [57]. Type I is

involved in translational regulation and type II in transcriptional regulation [84, 86]. Both

types of aptamers are H-type pseudoknots, but for type II the presence of a ligand causes

conformation changes when bonded [85]. For example, in *Bacillus subtilis* when PreQ$_1$

binds to the ligand, the riboswitch folds into an H-type pseudoknot [58]. This folding

causes a conformational change into a terminator hairpin. PreQ$_1$ bonded with the ligand is

considered "ON" and gene expression is terminated in this situation. When the ligand is

not bonded, the riboswitch is "OFF", and gene expression continues.

In this research, the aptamer domain was changed in different forms. This

followed the process that was used in the article, Rational Re-engineering of a

Transcriptional Silencing PreQ$_1$ Riboswitch [53]. In this study, three different

riboswitches were created from PreQ$_1$. Figure 3 shows the aptamer domain of PreQ$_1$. The

aptamer domain for this riboswitch has one loop shown. When re-engineering this, the

loop had to be sustained.

Figure 3. Structure of PreQ1 Aptamer [53]

2.3 Biomarkers

"A defined characteristic that is measured as an indicator of normal biological processes, pathogenic processes, or responses to an exposure or intervention, including therapeutic interventions. Molecular, histologic, radiographic, or physiologic characteristics are types of biomarkers [69]." This is a general definition of biomarkers from the American National Institute of Health (NIH) and the Food and Drug Administration (FDA). Types of biomarkers are hormones, neurotransmitters, enzymes,

and metabolites [17, 74]. Biomarkers can range is size and weights as they are made up

of molecules of different sizes [69]. Depending on these factors, riboswitch aptamers can

bind based on their affinities for each biomarker [14, 48]. If there is a high concentration

of a biomarker, a riboswitch aptamer could bind to it and a conformational change would

occur. This would lead to the expression platform of the riboswitch to react. As stated

above, an expression platform would then have multiple different responses based on the

bonding. The image below shows how biomarker react with different areas of the body,

Figure 4. This will be discussed in the specific biomarker sections as well.
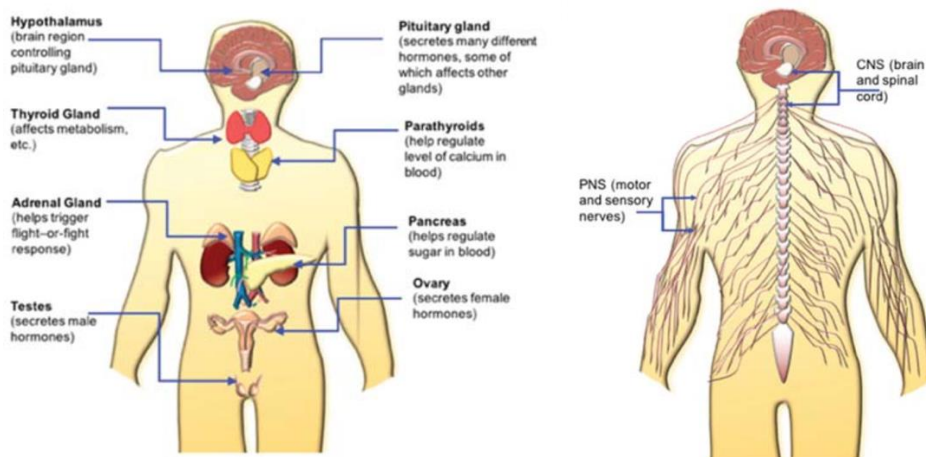
Figure 4. Anatomical schematic of endocrine and nervous systems [69]

In the article, Stress Biomarkers in Biological Fluids and Their Point-of-Use

Detection, stress biomarkers are described [69]. For hormones and neurotransmitters,

biomarkers are involved with the endocrine and nervous systems. As stress is a hormone

biomarker, the article explains how stress affects the body and travels when released. The

article talks about a general observation of biomarkers. These biomarker concentrations range over 6 orders, higher concentrations usually lead to smaller molecules, molecular weight tends to decrease the concentration [69]. Some of the most common biomarkers are serotonin, dopamine, and cortisol [87].

Cortisol has shown to play a positive role in physical performance [20]. As stated in the article, cortisol is involved in catabolic metabolism. A ratio of cortisol with testosterone can be used as a tool to detect overtraining. In this article, soccer players were tested after a tournament, players did performance testing and then gave blood and saliva samples [20]. The results from this study showed that biomarkers had correlations to hematological, inflammatory, and endocrinological markers. This test did have limitations to sample size, age, and category. Markers that were looked at in this study that showed to be significant were cortisol, testosterone, creatine kinase, sex hormones, cytokines, hematological panels, and nutritional markers. Creatine kinase is a biomarker for skeletal muscle damage. This marker should increase after a training session. Cortisol and testosterone are usually looked at for prolonged physical stress. By looking at a panel of multiple biomarkers, performance could be examined [18].

Biomarkers are described in, Biomarkers of physical activity and exercise [16]. Cortisol, testosterone, lactate, creatine kinase, creatinine, ammonia, lactate dehydrogenase, uric acid, urea, homocysteine, cardiac troponin, malondialdehyde and protein carbonyls, superoxide dismutase and glutathione peroxidase, reactive oxygen species, C-reactive protein, interleukin-6, and leukocytes are explained in this article.

They are broken down through areas of the body they affect [38]. Biomarkers also have

chemical background within the body [25]. Solubility is based on the molecular structure

of the biomarker.

Biomarkers that are used in this study are Cortisol, Serotonin, Dopamine,

Epinephrine, Norepinephrine, and DHEA-S. Each of these biomarkers will be briefly

described along with their chemical structure.

2.4 Cortisol

Cortisol is released from adrenal glands through activation of the hypothalamic-

pituitary-adrenal axis [11]. It is a glucocorticoid steroid hormone with the primary

function to increase blood sugar. It does this through the process of gluconeogenesis [66].

The chemical structure of cortisol is shown below in Figure 5.
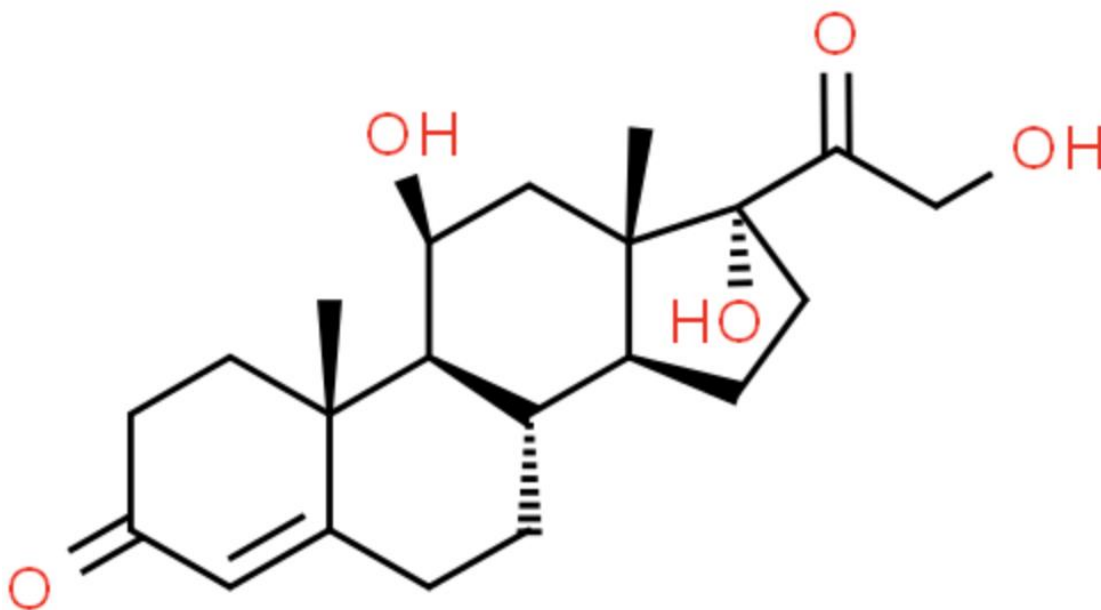
Figure 5. Chemical structure of cortisol

Cortisol is known to be a biomarker for stress. An acute high level of cortisol is used for survival. Prolonged stress or high levels of stress can deteriorate the body and cause physiological problems. These situations are where cortisol is at a chronic high level. Mental issues can arise from chronic high levels of cortisol as well.

2.5 Serotonin

Serotonin has various roles like vascular resistance and blood pressure. It also can be related to virtually all major organ systems. Serotonin is produced in the central nervous system [77]. The chemical structure of serotonin is shown below in Figure 6.
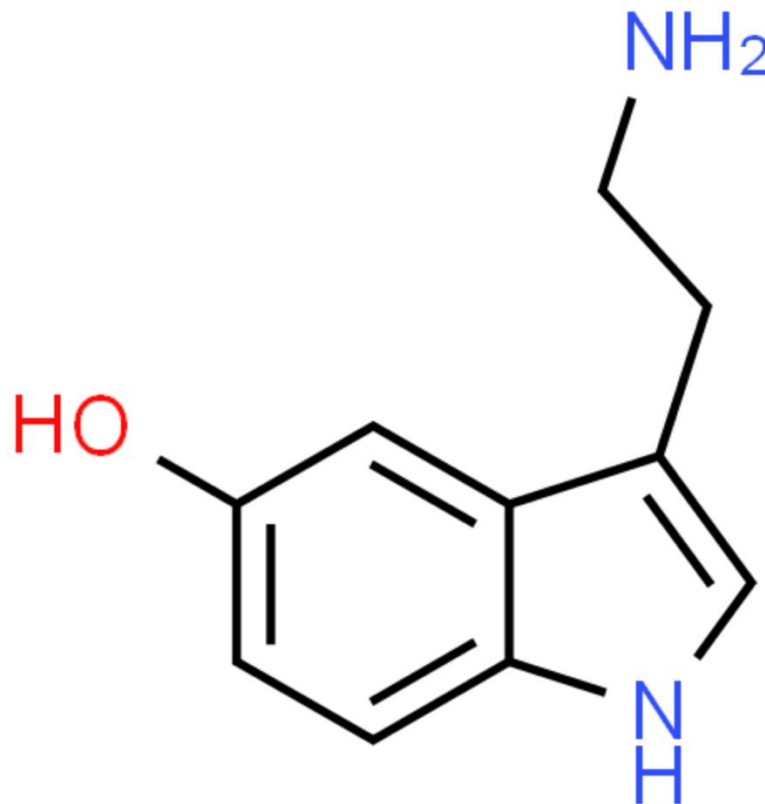
Figure 6. Chemical structure of serotonin

Serotonin regulates behavioral and neuropsychological processes such as mood, perception, reward, anger, aggression, appetite, memory, sexuality, and attention. Mental illnesses like anxiety are treated through drug that target serotonin receptors.

2.6 Dopamine

Dopamine can be seen in many roles in the body. The dopaminergic system is when dopamine is involved as a neurotransmitter. This system plays roles neuromodulation and influences different immune systems [30]. For neuromodulation the following are included: movement and motor control, spatial memory function, motivation, arousal, reinforcement, reward, sleep regulation, attention, affect, cognitive function, feeding, olfaction, and hormone regulation. Immune systems that are involved are cardiovascular, gastrointestinal, and renal. The chemical structure of dopamine is shown below in Figure 7.
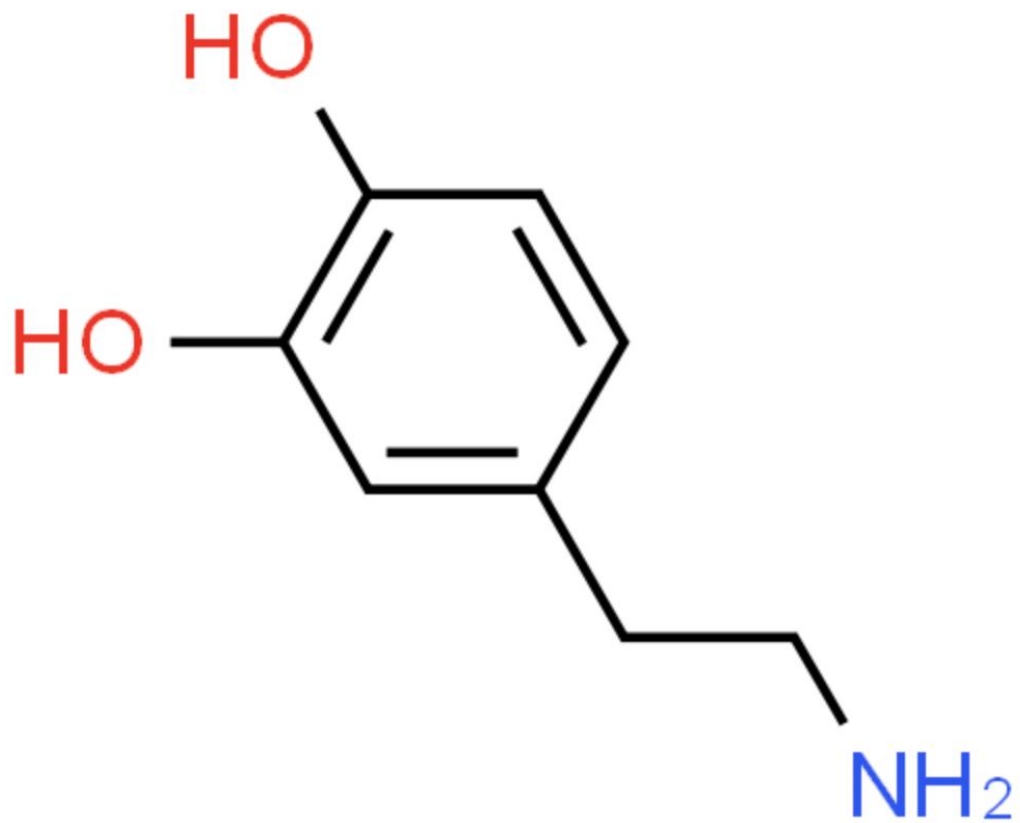
Figure 7. Chemical structure of dopamine

2.7 Epinephrine & Norepinephrine

Epinephrine and norepinephrine are synthesized from dopamine. They both bind to adrenergic receptors [55]. Epinephrine has a fast and short stress-response signal. These two differ by a methyl group on the nitrogen side chain. This is shown in the figures below, the chemical structures for both are shown.
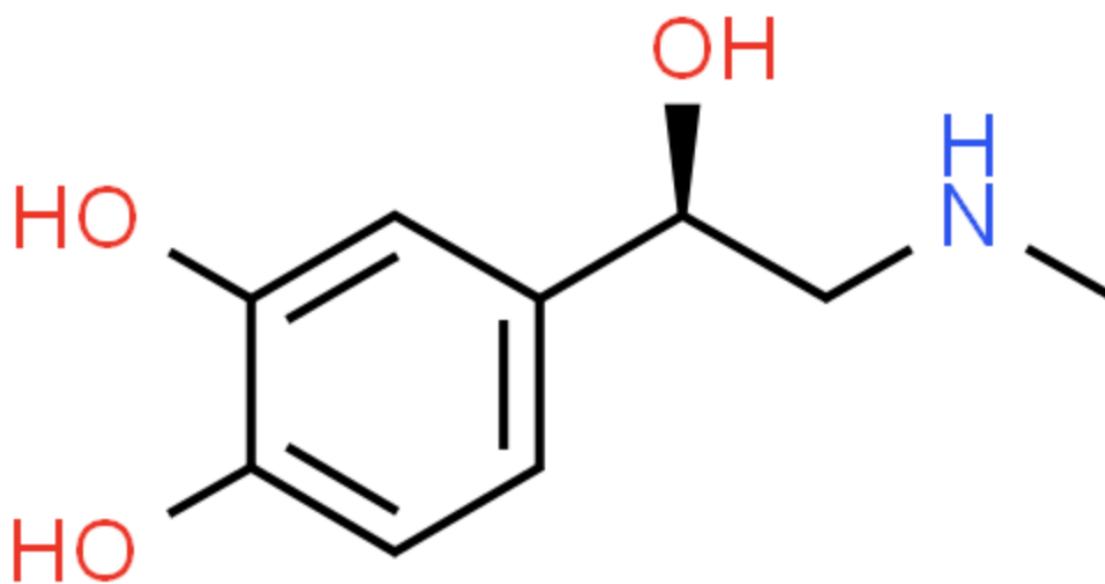
Figure 8. Chemical structure of epinephrine
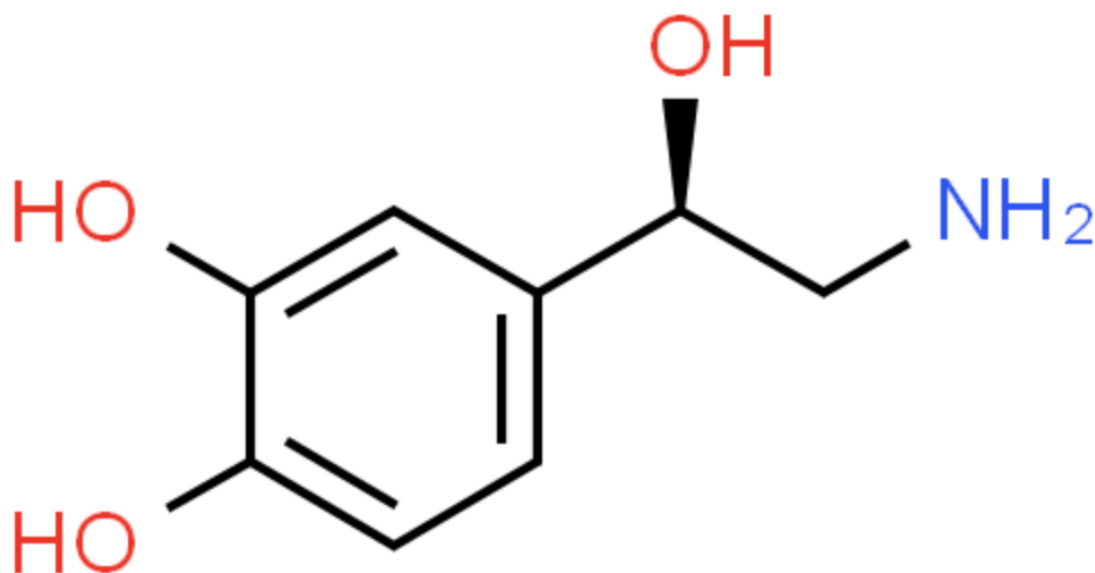
Figure 9. Chemical structure of norepinephrine

2.8 DHEA-S

DHEA-S is produced by the adrenal glands in women and men. It is a protective anabolic hormone with its role of maintaining and restoring the human body. The chemical structure of DHEA-S is shown below in Figure 10.
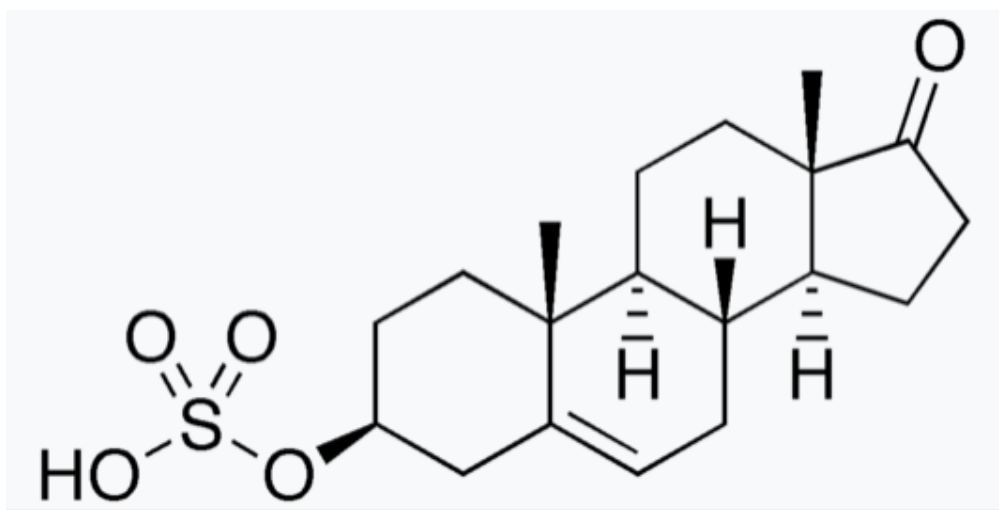
Figure 10. Chemical structure of DHEA-S

2.9 Reengineering Riboswitches

There are known methods for synthetically developing riboswitches and ligands [27]. One method is the SELEX (Systematic Evolution of Ligands by Exponential Enrichment) [22, 88]. This is an in vitro selection method commonly used for aptamers [73]. The SELEX method consists of three steps: selection, portioning, and amplification [9]. This is shown in the below image, Figure 11.
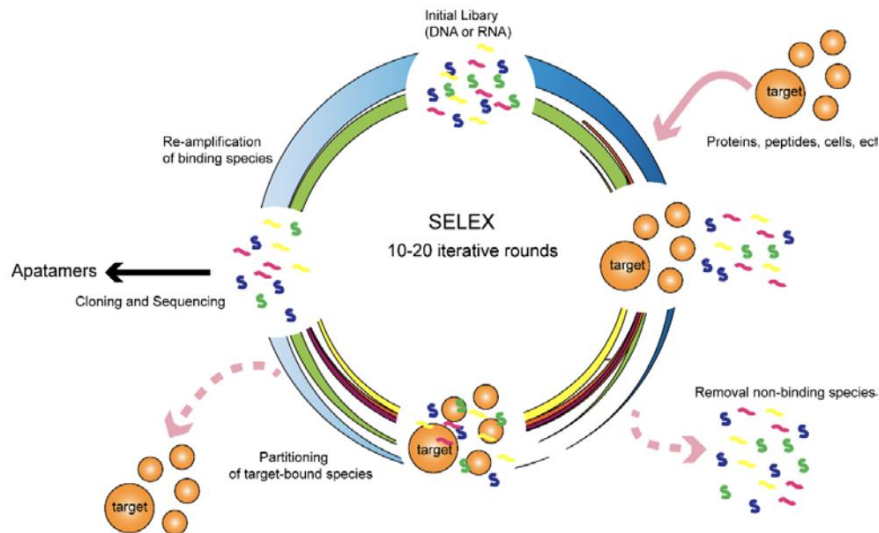
Figure 11. Schematic illustration of the SELEX process for the DNA and RNA library

Methods involving engineering riboswitches varies for each type. One method that took a natural reengineer path over creating a synthetic riboswitch is in the article [34]. A secondary structure was created with biological sources that host multiple aptamers [34]. The purpose of this research was to create a riboswitch that would, when bonded with the ligand, turn "ON". The article mentions using natural RNA elements has more advantages over computational. Ceres et al. thought to bind a biological structure to the aptamer. This would then change the expression platform. The results for this research were extensive, due to the wide range of riboswitches that needed to be tested. As they wanted to engineer a natural "OFF" switch to be an "ON" switch, specific classes needed to be chosen. In the article, two modular "ON" switches were made [34]. One drawback from this research is that these methods can be referred to but will need major

adjustments for each riboswitch. A predictable regulatory system will most likely come

from in vivo research based on the article Computational analysis of riboswitch-based

regulation [24, 64].

A method that was used in Design of Mammalian ON-Riboswitches Based on

Tandemly Fused Aptamer and Ribozyme used twister ribozymes [28]. In this article, a

ribozyme and aptamer were "fused in tandem" and by fusing, it forms an aptazyme. This

structure can take on the form of only the ribozyme or the aptamer. Depending on the

form it takes, while being placed upstream of the aptamer, it will either turn the

riboswitch in an "ON" or "OFF" form [10]. This article was submitted in 2019 and within

recent literature, ribozymes/aptazymes have become popular in research on riboswitches.

A guanine aptamer was experimented with a twister ribozyme [28]. The results show that

based on the stability of the aptamer dictates whether the aptazyme will take on the

characteristics of the aptamer of ribozyme. This article shows a different method than

Ceres et al. and one major difference is the use of ribozymes. Ceres et al. method was to

bind to biological elements, ribozymes were not used. The same problem does arise in

Mustafina et al. research like Ceres et al. by each riboswitch will need different methods

and new experimentation.

Alternately, *Automated physics-based design of synthetic riboswitches from*

diverse RNA aptamers, uses a computational approach. The approach that was taken in

this article stems from experimental aptamers not being transitioned to functional

riboswitches [12]. This is due to "the qualitative design by experts, combinatorial library

generation and high- throughput screening" Though this article is not looking at re-engineering a riboswitch, it is finding a computational model to predict the function of the riboswitch. Espah Borujeni et al. validated 77 synthetic riboswitches with diverse aptamers [12]. Through measuring free energy, equations were created and proven to predict riboswitch activation [50]. Using the model, an algorithm was created to convert RNA aptamers into synthetic riboswitches. This research statistically finds different RNA aptamers and can create a functional riboswitch through modeling [65]. One restriction to this research is that the research is computational and not tested on bacteria culture. The article states the model assumes thermodynamic equilibrium between the ribosome, mRNA, and ligand [12]. Computational is a good way to start the research, but without predicting mRNA stability it can't be put in place. In *Computational analysis of riboswitch-based regulation*, they agree that using a computational model is the best way to predict a riboswitch structure. It also mentions that when a computational model is used in conjunction with functional evidence, it is more powerful in detecting regulatory sequences [24].

Through the research discussed above, a computational design followed by laboratory procedure is supported [29]. A computational design saves resources by creating a base design [59]. The common method seen is a mix and match of computational design and laboratory procedures. By having software as a preliminary output for that method, less laboratory trials would be needed. A laboratory follow up can

then test the riboswitch for how it responds. These two methods can also then be compared, for how the energy levels differ.

3. Methodology

3.1 Experimental design:

The experimental design for this research was to create riboswitch designs for PreQ$_1$ computational through the programs KineFold and NUPACK. Four riboswitch strands were created, and three riboswitch strands were from research [53] to test as well. These strands were then prepared to test against the original PreQ$_1$ strand with different biomarkers. This is further explained below.

3.2 Riboswitch structure modeling:

Computational biology was used to predict riboswitch behavior with different variant sequences. NUPACK and KineFold were software's that provided data for these predictions. These computational models were used by inserting an RNA sequence and outputting different statistics on each sequence. Using those statistics. Predictions could be made with how the experimental results could respond.

Riboswitch variants were designed, based on the aptamer layout for PreQ$_1$. Variants 1-4 were designed to have 22 nucleotides and be able to design a loop compared to the original in KineFold. By exchanging different nucleotides in the original, each variant was created. Figure 13-16 shows the KineFold simulations, which were compared to the original in Figure 12. KineFold shows the Free energy of each simulation and is shown on the bottom of the figures. Variants 5-7 were pulled from the cited research. Table 5 shows the sequences of each variant.
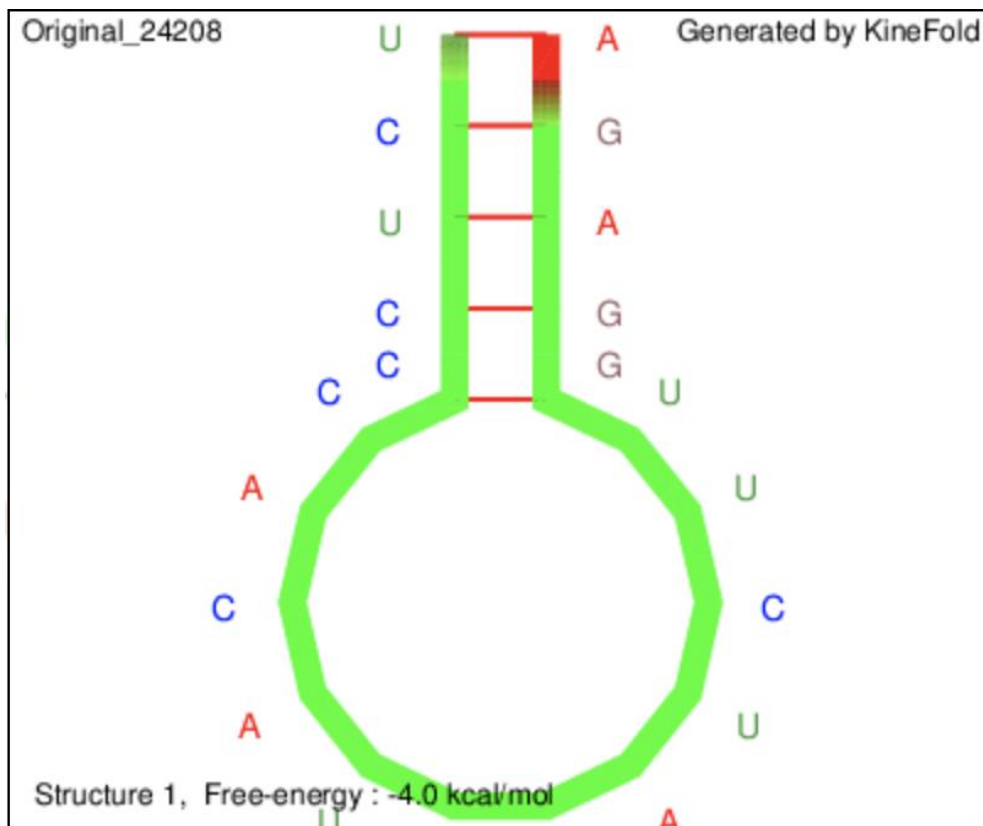
Figure 12. PreQ₁ riboswitch simulation made on KineFold
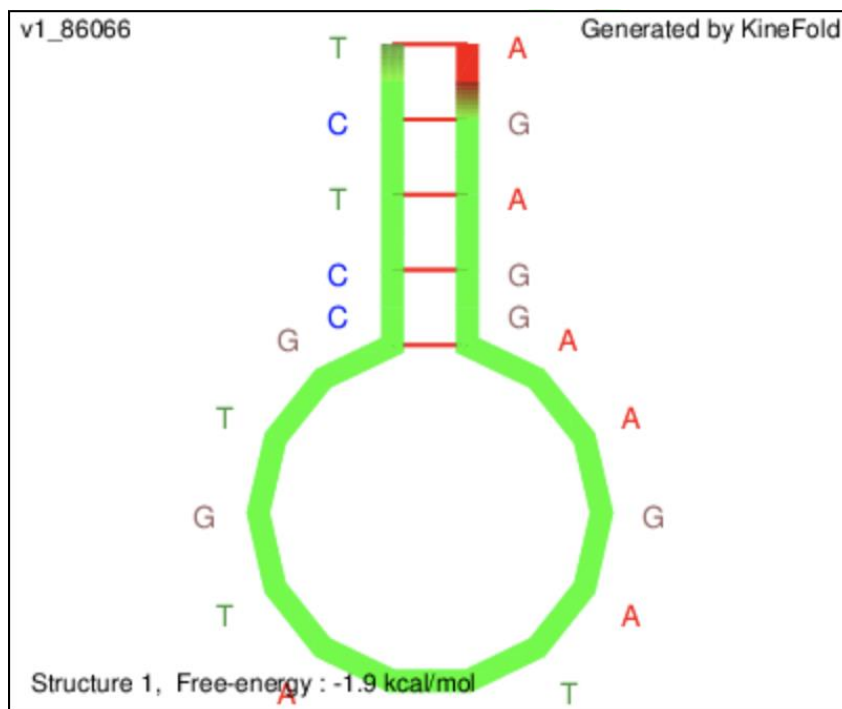
Figure 13. Variant 1 simulation made on KineFold
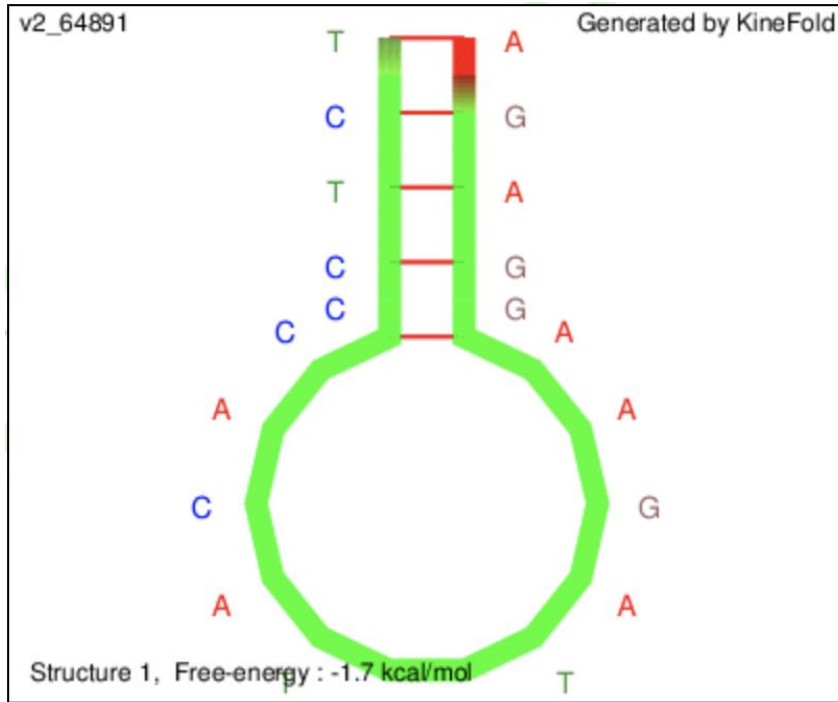
Figure 14. Variant 2 simulation made on KineFold
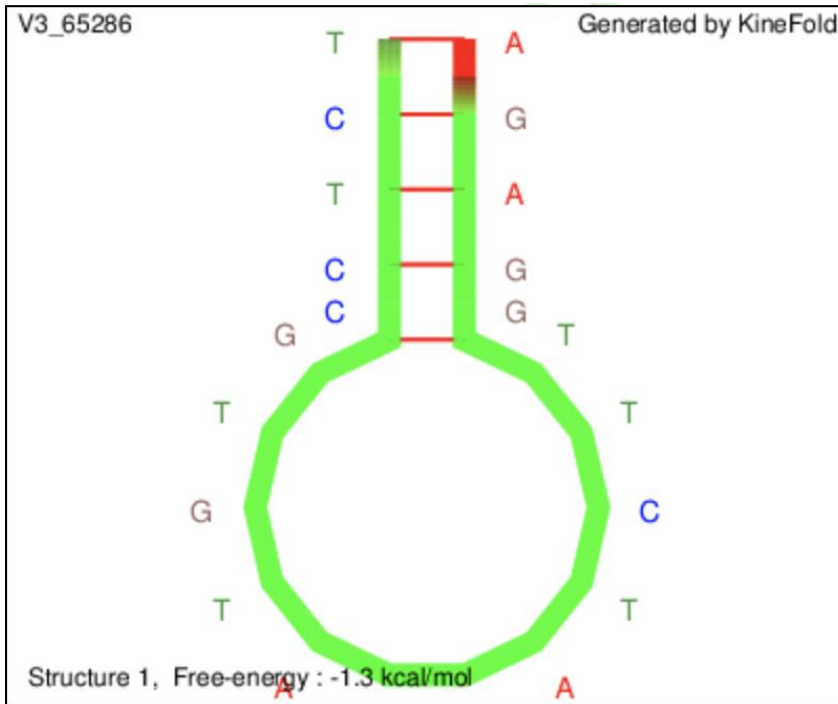
Figure 15. Variant 3 simulation made on KineFold
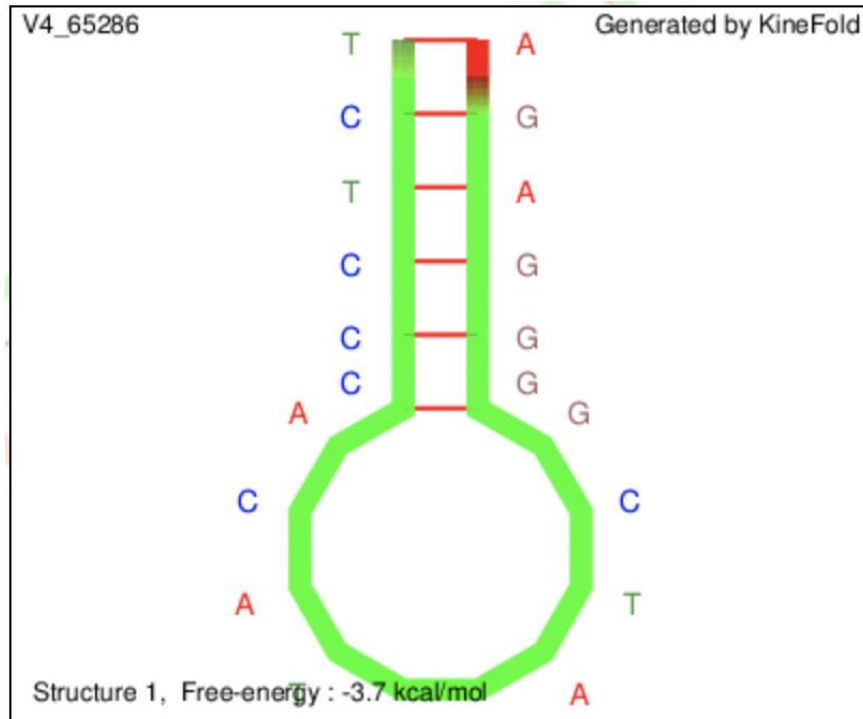
Figure 16. Variant 4 simulation made on KineFold

3.3 Plasmid constructs:

All plasmids were constructed by isothermal (Gibson) assembly using NEBuilder HiFi

DNA Assembly Master Mix (New England Biolabs, Ipswich, MA). PCR primers and

gBLOCK DNA fragments (serving as DNA templates) were obtained from Integrated

DNA Technologies (Coralville, IA). Plasmid manipulations were performed using MAX

Efficiency DH5α chemically competent E. coli cells (Invitrogen, Carlsbad, CA).

Plasmid pPreQ1-sfGFP: The plasmid pJBL7010 (Addgene, Watertown, MA) containing

sfGFP encoding sequence under control of bacterial J23119 promoter was used to insert

PreQ1 riboswitch sequence and create the plasmid pPreQ1-sfGFP. The plasmid

pJBL7010 was linearized by using PCR with forward (5'-

ATGAGCAAAGGTGAAGAACTGTTTACC-3') and reverse (5'-

ACTAGTATTATACCTAGGACTGAGCTAGCTGTCAA-3') primers. PreQ1

riboswitch sequence was amplified in PCR reaction from a single stranded DNA

fragment (5'-

AAGTGAAAAAATTGAAGAAAATCCGTGCGATATGCGGGAGAGGTTCTAGCTA

CACCCTCTATAAAAAACTAAGGACGAGCTGTATCCTTGGATACGGCCTTTTTT

CGTTATGGCAGGAGCAAACT-3') using forward (5'-

CTCAGTCCTAGGTATAATACTAGTAAGTGAAAAAATTGAAG-3') and reverse

(5'- GTTCTTCACCTTTGCTCATAGTTTGCTCCTG-3') primers. PCR allows the

addition of overlapping sequences (underlined) (required for Gibson Assembly-based

ligation) to the ends of amplified products. Both PCR reactions were performed in 50 µl

volume using 1 ng/µl DNA template (pJBL7010 or PreQ1 DNA fragment), 0.2 µM

primers, 200 µM dNTPs, 1X HF Buffer (New England Biolabs, Ipswich, MA), 3%

DMSO, and 0.5 µL (1.0 units) Fusion High-Fidelity DNA Polymerase (New England

Biolabs, Ipswich, MA). The PCR reactions were performed in thermocycler using

conditions presented in Table 2 and Table 3.

Table 2. Thermocycling conditions for amplification of pJBL7010.

Number of Cycles	Program
1	98 ℃ for 30 s
29 cycles	98 ℃ for 10 s, 53 ℃ for 30 s, 72 ℃ for 5
1	s
End	72 ℃ for 10 min
	4 ℃

Table 3. Thermocycling conditions for amplification of PreQ1 sequence.

Number of Cycles	Program
1	98 ℃ for 30 s
29 cycles	98 ℃ for 10 s, 53 ℃ for 30 s, 72 ℃ for 5
1	s
End	72 ℃ for 10 min
	4 ℃

PCR products were analyzed by standard 1% agarose gel electrophoresis (Figure 17). 0.5

g agarose were added to 50 mL 1X Tris-Acetate-EDTA (TAE) buffer (Fisher Scientific,

Pittsburg, PA). The solution was boiled on the hotplate stirrer to dissolve the agarose.

The solution was cooled to approximately 50 °C and 3 μL of SYBR® Safe DNA Gel

Stain (Invitrogen, Carlsbad, CA) were added. The melted agarose was poured into a gel

tray with the well comb in place. The gel was cooled at room temperature until it was

completely solidified. The comb was removed and the tray with the gel was placed into

the electrophoresis box. The gel box was filled with 1X TAE buffer until the gel is

covered. 10 μL of 2-Log DNA Ladder (New England Biolabs, Ipswich, MA) and

samples mixed with gel loading dye (New England Biolabs, Ipswich, MA) were loaded,

and the gel was ran at 130 V until the dye line is approximately 75–80% of the way down

the gel. The DNA fragments were visualized using the device with UV excitation,

Figure 17. Gel electrophoresis of DNA fragments visualized in UV excitation
PCR products were purified using MinElute PCR Purification Kit (Qiagen, Valencia,
CA).
Purified PCR products were ligated at 50 ℃ for 30 min using NEBuilder HiFi DNA

Assembly Master Mix (New England Biolabs, Ipswich, MA) (See Table 4).

Table 4. Gibson Assembly reaction.

Insert:Vector Molar Ratio	0.025:1
Linearized pJBL7010	3 µL (0.075 pmol)
PCR PreQ1	0.3 µL (0.225 pmol)
NEB Master Mix	10 µL
Water	6.7 µL

2 µL of the reaction were used to transform DH5α chemically competent E. coli cells (Invitrogen, Carlsbad, CA). Cells were thawed and gently mixed. 100 µL of competent cells were aliquoted to chilled polypropylene tubes. The ligated reactions were diluted 5-fold in 10mM Tris-HCL and 1mM EDTA 1 µL of dilution was added to the cells. The cells were incubated for 30 minutes, then heat shocked for 45 seconds in 42ºC water bath, then placed on ice for 2 minutes. 0.9 mL of room temperature S.O.C. Medium (Cat. No. 15544-034) was added. The cells were then shaken at 225rpm (37ºC) for 1 hour. The cells were grown overnight on LB-agar plates supplemented with antibiotic (100 μg/mL of ampicilline). Formed colonies were picked from the plate, and each colony was transferred into 5 mL of LB media supplemented with antibiotic and grown overnight. The cells were collected by centrifugation; and plasmids were purified using QIAprep Spin Miniprep Kit (Qiagen, Valencia, CA). The sequences of purified plasmids were verified by DNA sequencing (Eurofins Genomics LLC, Louisville, KY). The plasmid map of the resulting construct (pPreQ1-sfGFP) is shown in Figure 18.
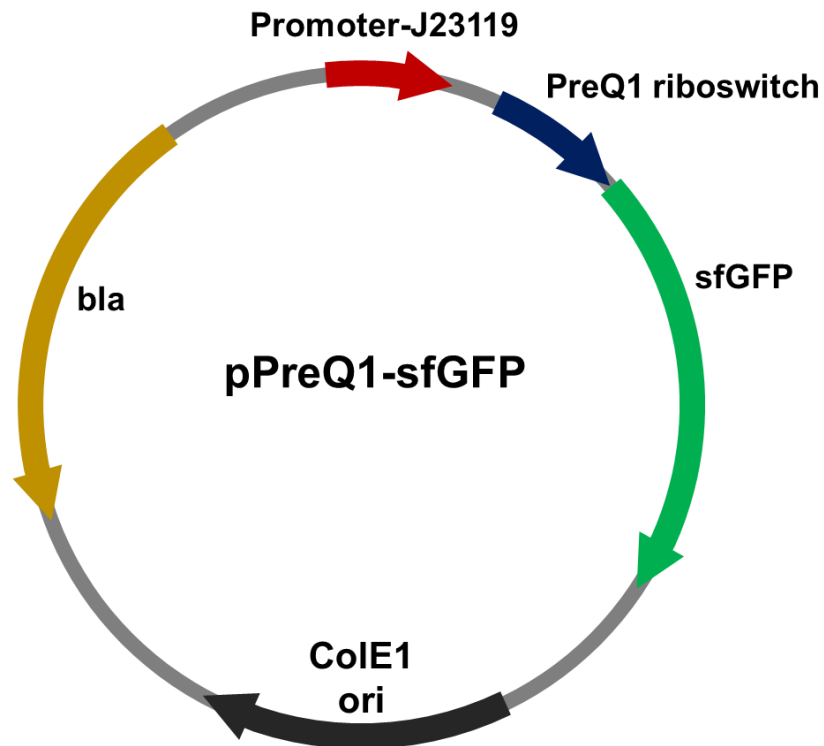
Figure 18. Plasmid map of pPreQ1-sfGFP. The plasmid contains PreQ1 riboswitch sequence placed upstream of sfGFP encoding gene under control of bacterial J23119 promoter, β-lactamase encoding gene (bla) responsible for resistance to ampicillin.

Plasmid pPreQ1 variant-sfGFP. To create plasmids containing PreQ1 riboswitch variants upstream of sfGFP encoding pJBL7010 was linearized as described above. Each of PreQ1 riboswitch variant sequence was amplified in PCR reaction from a single stranded DNA template using forward (5'-CTCAGTCCTAGGTATAATACTAGTAAGTGAAAAAATTGAAG-3') and reverse (5'- GTTCTTCACCTTTGCTCATAGTTTGCTCCTG-3') primers. Full description of DNA templates is presented in Table 5.

Table 5. Sequences of DNA templates for amplification of PreQ1 riboswitch variants

Riboswitch variant	DNA template
1	AAGTGAAAAAATTGAAGAAAATCCGTGCGATATGCGGGAGAGGAAGATCGATGTGCCTCTATAAAAAACTAAGGACGAGCTGTATCCTTGGATACGGCCTTTTTTCGTTATGGCAGGAGCAAACT
2	AAGTGAAAAAATTGAAGAAAATCCGTGCGATATGCGGGAGAGGAAGATCCTACACCCTCTATAAAAAACTAAGGACGAGCTGTATCCTTGGATACGGCCTTTTTTCGTTATGGCAGGAGCAAACT
3	AAGTGAAAAAATTGAAGAAAATCCGTGCGATATGCGGGAGAGGTTCTAGGATGTGCCTCTATAAAAAACTAAGGACGAGCTGTATCCTTGGATACGGCCTTTTTTCGTTATGGCAGGAGCAAACT
4	AAGTGAAAAAATTGAAGAAAATCCGTGCGATATGCGGGAGAGGGGCTATCTACACCCTCTATAAAAAACTAAGGACGAGCTGTATCCTTGGATACGGCCTTTTTTCGTTATGGCAGGAGCAAACT
5	AAGTGAAAAAATTGAAGAAAATCCGTGCGATATGCGGGAGAGGTTCTAGCTACATCCTCTATAAAAAACTAAGGACGAGCTGTATCCTTGGATACGGCCTTTTTTCGTTATGGCAGGAGCAAACT
6	AAGTGAAAAAATTGAAGAAAATCCGTGCGATATGCGGGAGAGGTTCTAGTTACACCCTCTATAAAAAACTAAGGACGAGCTGTATCCTTGGATACGGCCTTTTTTCGTTATGGCAGGAGCAAACT
7	AAGTGAAAAAATTGAAGAAAATCCGTGCGATATGCGGGAGAGGTTCTAGTTACATCCTCTATAAAAAACTAAGGACGAGCTGTATCCTTGGATACGGCCTTTTTTCGTTATGGCAGGAGCAAACT

PCR reactions were performed in 50 µl volume as described above. The equipment used and the PCR products are shown in Figures 19 & 20 respectively. The thermocycling conditions are presented in Table 6.

Figure 19: Thermocycler used through Wright Patterson Air Force Base
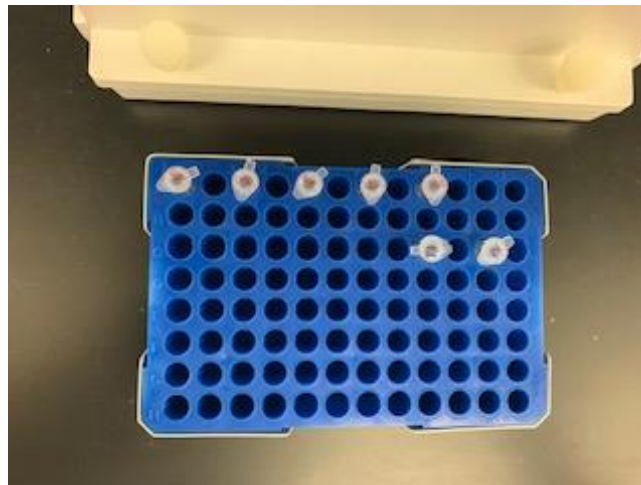
Figure 20: PCR Products

Table 6. Thermocycling conditions for amplification of PreQ1 riboswitch variants.

Number of Cycles	Program
1	98 ºC for 30 s
29 cycles	98 ºC for 10 s, 53 ºC for 30 s, 72 ºC for 5 s
1	
End	72 ºC for 10 min
	4 ºC

PCR products were analyzed by standard 1% agarose gel electrophoresis (See Figure 21 & 22).
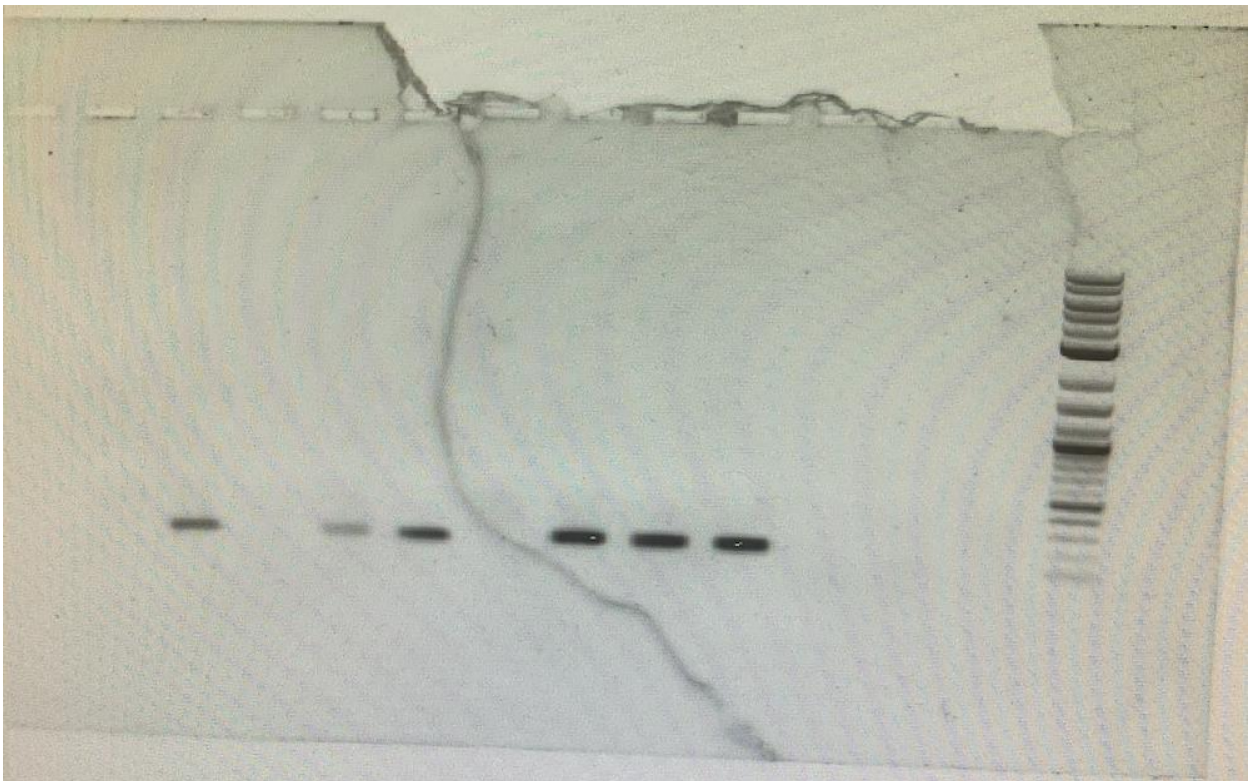
Figure 21. Gel electrophoresis of variant amplifications
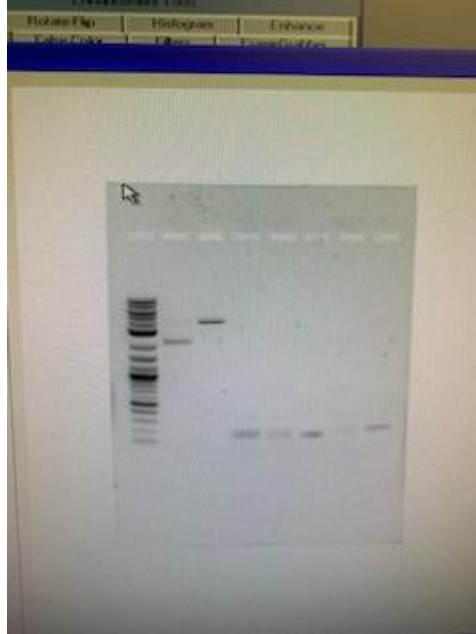
Figure 22: Gel Electrophoresis of PreQ$_1$ amplification

Purified PCR products were ligated at 50 ℃ for 30 min using NEBuilder HiFi DNA

Assembly Master Mix (New England Biolabs, Ipswich, MA) (See Table 7).

Table 7. Gibson Assembly reaction.

Insert:Vector Molar Ratio	0.025:1
Linearized pJBL7010	3 µL (0.075 pmol)
PCR PreQ1 variant	0.3 µL (0.225 pmol)
NEB Master Mix	10 µL
Water	6.7 µL

2 µL of each reaction were used to transform DH5α chemically competent E. coli cells

(Invitrogen, Carlsbad, CA) as described above. The cells were grown overnight on LB-

agar plates supplemented with antibiotic (100 µg/mL of ampicillin). Formed colonies

were picked from the plates, and each colony was transferred into 5 mL of LB media

supplemented with antibiotic and grown overnight. The cells were collected by

centrifugation; and plasmids were purified using QIAprep Spin Miniprep Kit (Qiagen,

Valencia, CA). The sequences of all constructs have been verified by DNA sequencing at

the Eurofins Genomics LLC (Louisville, KY). See Figures 23 & 24 for formed colonies.
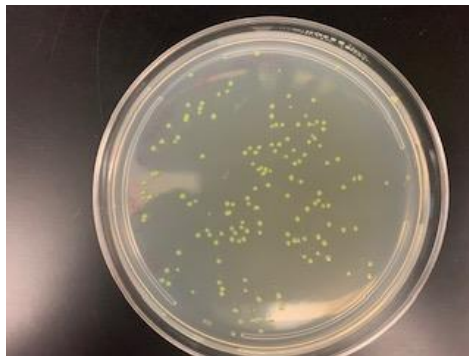
Figure 23: Formed colonies from Gibson Assembly

Figure 24: Formed colonies from Gibson Assembly under UV Excitation

3.4 Cell- free extract and cell- free reactions:

Cell extract and reagents were prepared based on previously described methods and were provided by the AFRL mentor. The final cell-free reaction based on S12 extract was composed of the following reagents: 8 mM magnesium glutamate; 10 mM ammonium glutamate; 130 mM potassium glutamate; 1.2 mM ATP; 0.850 mM each of GTP, UTP, and CTP; 0.034 mg/mL folinic acid; 0.171 mg/mL yeast tRNA; 2 mM amino acids; 30 mM PEP; 0.33 mM NAD; 0.27 mM CoA; 4 mM oxalic acid; 1 mM putrescine; 1.5 mM spermidine; 57 mM HEPES; 30% S12 extract by volume; plasmid DNA 20 ng/µL and water.

To activate the riboswitch, cell-free reactions were treated with appropriate concentrations of pre-queuosine1 dihydrochloride (PreQ1) in DMSO (see Results section). Equivalent volume of DMSO was added to the reactions for riboswitch in "OFF" state.

To test activation of riboswitch variants, cell-free reactions were treated with appropriate concentrations of cortisol or dehydroepiandrosterone sulfate (DHEAS) in DMSO or with appropriate concentrations of dopamine or norepinephrine in water. Equivalent volume of DMSO or water was added to the reactions for riboswitch in "OFF" state.

All cell-free reactions were prepared on ice in triplicates at the 12 µL scale. 45 µl of a mixture containing the desired reaction components was prepared and the 12 µL was pipetted into three wells of 384-well clear bottom black walled plate (Corning), taking care to avoid bubbles. The plate was sealed with an oxygen impermeable membrane to prevent evaporation. Reactions were incubated for 18 hours at 30º C and monitored using

a SpectraMax Paradigm Plate Reader (Molecular Devices), measuring fluorescence every

10 minutes at 470 nm excitation and 510 nm emission wavelengths for sfGFP.

4. Results & Discussion

4.1 Chemical Structure

The software NUPACK was used to simulate the chemical structure [90]. The input requirements are in terms of DNA sequence to output the structure and chemical properties. Figure 25 shows the simulated results for PreQ$_1$, by the software. In Figure 25, the structure of PreQ$_1$ is shown on the left column showing the identity and the equilibrium probability for each position whereas the right column in this figure shows the helicity of this aptamer. The different nucleotides, A, C, G, and T, form the loop shown in Figure 25 and based on their sequence determines hydrogen bonding, equilibrium probabilities, and potential ligand binding [46]. The DNA configuration can be broken down into loops, which are scored in terms of free energy. In Figures 25 and 26, the free energy that is stated is the sum of the secondary loops. The secondary loops impact ligand bonding. The probability shown is the probability of the sequence to be in that formation. The ensemble defect is the average number of nucleotides that are incorrectly paired. For this number, 0 is the best and N would be the worst. Normalized ensemble defect is the percentage of this with 0% being the best and 100% being the worst. PreQ$_1$ will be the structure that the variants will be compared to, as PreQ$_1$ is already an established riboswitch.
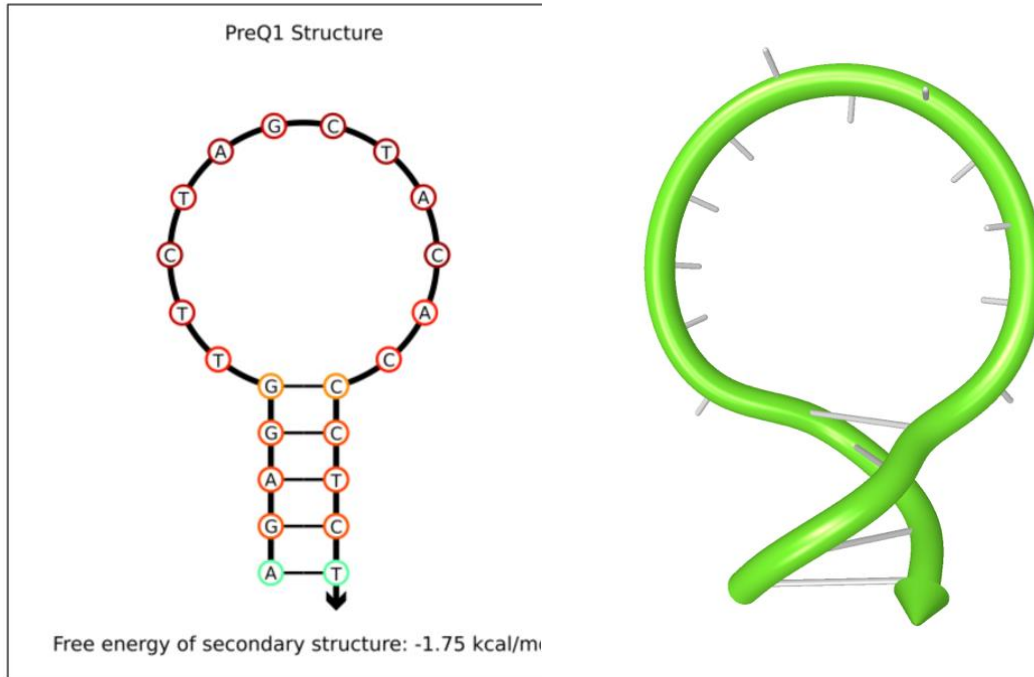
Figure 25. NUPACK simulation of PreQ₁ with identity and equilibrium probability shown to the left. To the right shows the helicity.

Figure 26. Structure properties for PreQ₁ made by NUPACK

As it is shown, the PreQ$_1$ structure has strong equilibrium probabilities throughout the

loop. In the details it shows that 22 nucleotides are being examined in the aptamer

domain. The details also show that there is a 0.326 probability that aptamer domain

would present this way. A 15.3% normalized ensemble defect is also shown through this

design structure. These details are then compared to the structures that were designed to

loop this way versus a design where it naturally occurs.

In addition to simulating the free energy structure, NUPACK can take input on

the structure. This allows for riboswitches to be designed and show the properties for the

structure. In the following figures, Figures 27-34, each variant is shown and was designed

how PreQ$_1$ is naturally. The properties are shown for each design in Figures 28, 30, 32,

and 34.
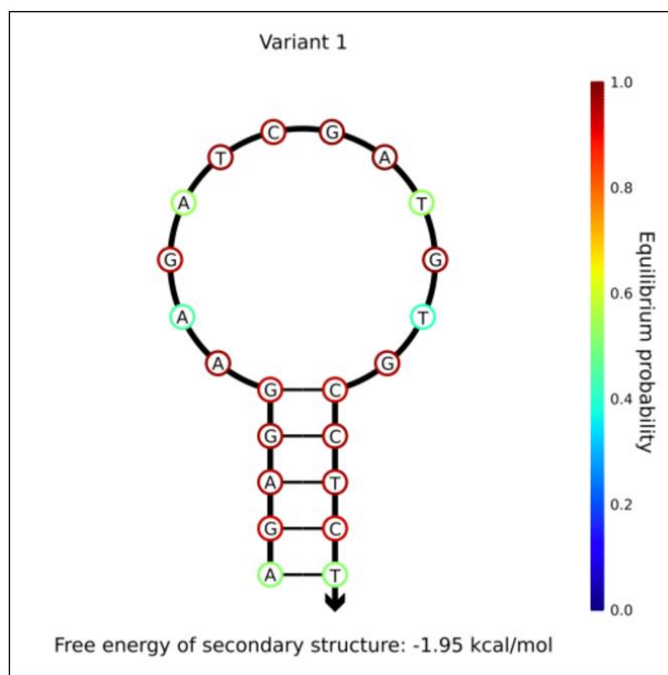
Figure 27. NUPACK design of Variant 1 with identity and equilibrium.

Details

Sequence properties ❓

Free energy:		−3.04	kcal/mol	❓
Base	Number	%		
A	6	27.3	❓	
C	4	18.2	❓	
G	7	31.8	❓	
T	5	22.7	❓	
Other	0	0.0	❓	

Sequence/structure properties ❓

Free energy:	−1.95	kcal/mol	❓
Probability:	0.170		❓
Ensemble defect:	3.5	nt	❓
Normalized ensemble defect:	16.0	%	❓
Nucleotides:	22	nt	❓

Figure 28. Structure properties for Variant 1 made by NUPACK

Free energy of secondary structure: -1.85 kcal/mol
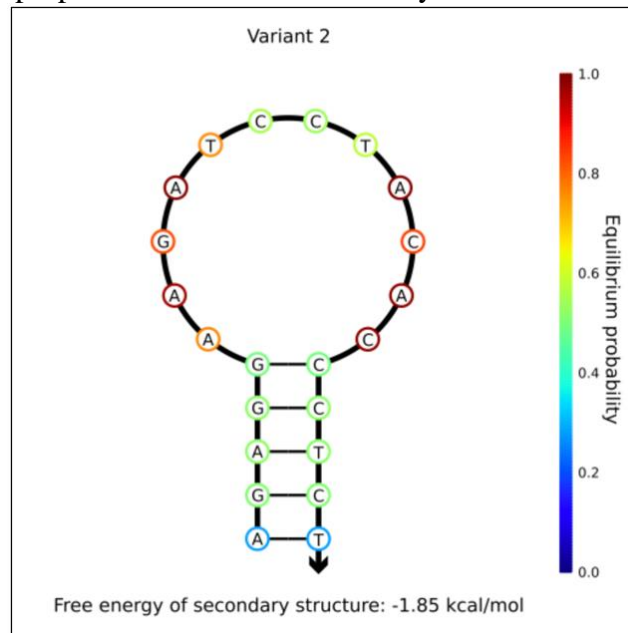
Figure 29. NUPACK design of Variant 2 with identity and equilibrium.

Figure 30. Structure properties for Variant 2 made by NUPACK
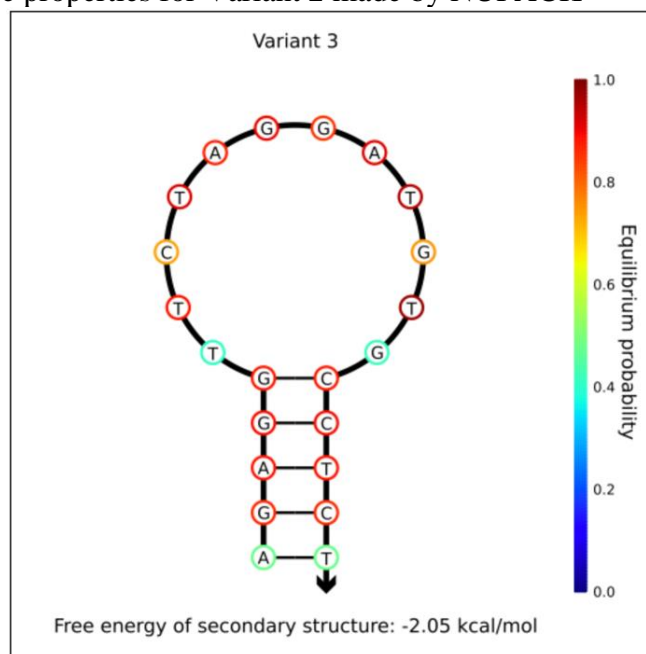
Figure 31. NUPACK design of Variant 3 with identity and equilibrium.

Figure 32. Structure properties for Variant 3 made by NUPACK
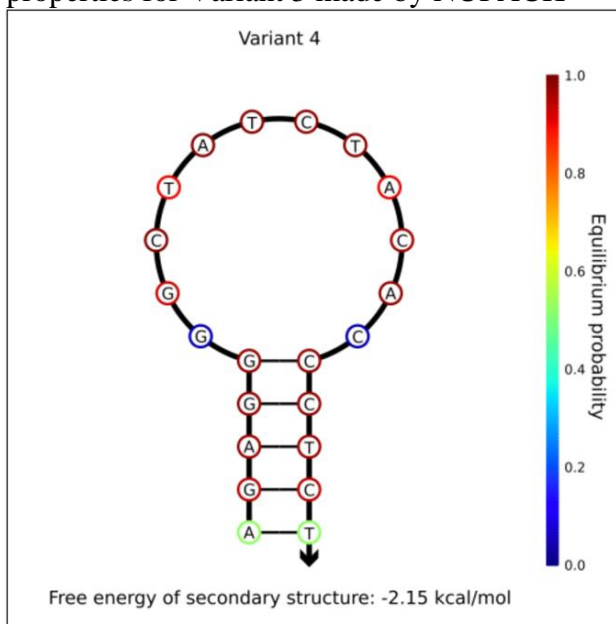
Figure 33. NUPACK design of Variant 4 with identity and equilibrium.

Details					
Sequence properties ❓			**Sequence/structure properties** ❓		
Free energy:	−4.71 kcal/mol ❓		Free energy:	−2.15 kcal/mol ❓	
Base	Number	%	Probability:	0.016	❓
A	5	22.7 ❓	Ensemble defect:	3.4 nt	❓
C	7	31.8 ❓	Normalized ensemble defect:	15.3 %	❓
G	5	22.7 ❓	Nucleotides:	22 nt	❓
T	5	22.7 ❓			
Other	0	0.0 ❓			

Figure 34. Structure properties for Variant 4 made by NUPACK

The results above show the four variant designs of PreQ$_1$ that were designed. The variants equilibrium probabilities show different probabilities than the original. Variants 1 and 2 are most different with multiple green and blue tones in Figures 27 and 29, indicating they have a lower probability of this structural formation. Variants 3 and 4 have differences in comparison to the original, but they keep to a closer probability as the original. From the equilibrium probability it is expected that variants 3 and 4 will respond similarly to PreQ$_1$.

The NUPACK result details for each structure provide the probability for the formation of each structure. For the original structure of PreQ$_1$ there is a 0.326 probability. For variant 1 the probability is 0.170, variant 2 the probability is 0.166, variant 3 the probability is 0.120, and variant 4 the probability is 0.016. For these details, the riboswitch aptamer is not bonded to a ligand. This means in the presence of a ligand; the probabilities could be different than a computational model. The probability equilibrium is more accurate, due to it being based on the pairing probabilities. The

46

closest probabilities to the original will most likely react similarly to a ligand. The following results are experimental results.

4.2 Riboswitch Activation Time Results

In this section, the results of each analyte tested against the original $PreQ_1$, and variants is shown (Figure 35-43). In each graph a line represents a riboswitch activation over time. The activation is measured by the excitation and emission fluoresce (excitation at 470nm and emission at 510nm). When the solution of the RNA mixture with either an analyte or control, the RFU value over time will have a linear trend. As the solution balances out and the ligand binds, the RFU plateaus. The following figures show this trend. The peak and plateau level depicts if the riboswitch is transcribing proteins or terminated.

A test was run for the riboswitch being OFF in water and DMSO for comparison with each analyte. $PreQ_1$, DHEA-S, and cortisol are compared against the OFF state with DMSO. The other biomarkers are compared against the OFF state with water. These graphs show the variants response with respect to the original design. The OFF state is when the aptamer is not bonded to a ligand. When the analyte is added, the riboswitch aptamer binds. The analyte or biomarker is the ligand in this occurrence. The riboswitch is then in an ON state. When no ligand is present, $PreQ_1$'s expression platform is transcribing, which explains the OFF state having higher relative fluorescence units (RFU). This is shown with the OFF (DMSO) having a peak around $2.50*10^7$ and $preQ_1$ is close to zero.

47
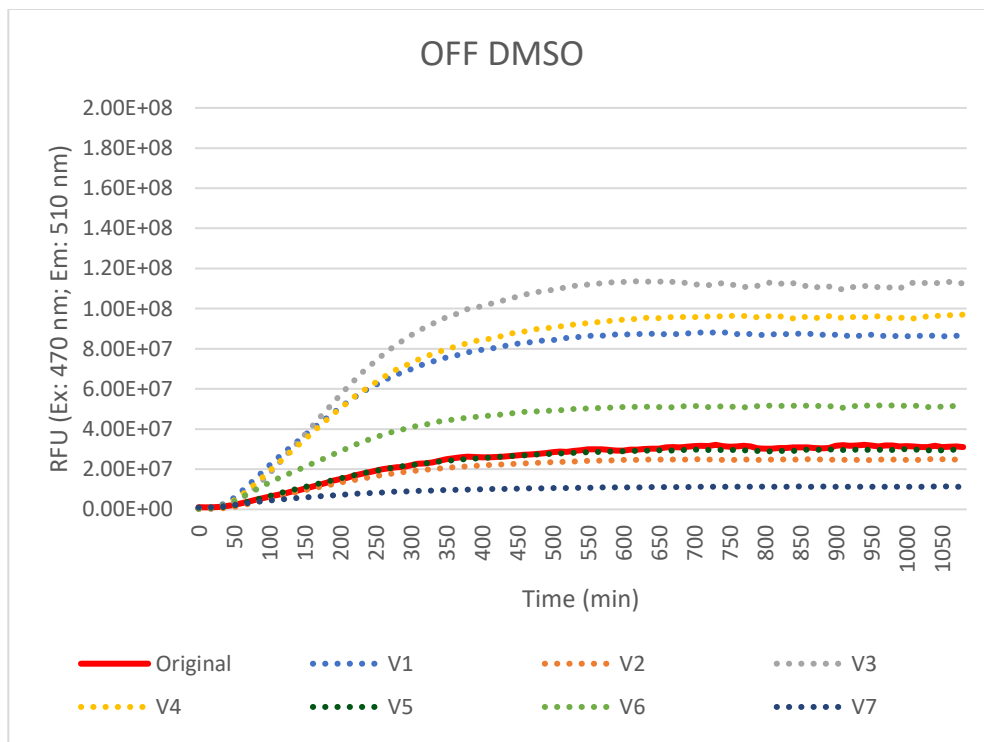
Figure 35. Riboswitch time log with OFF DMSO
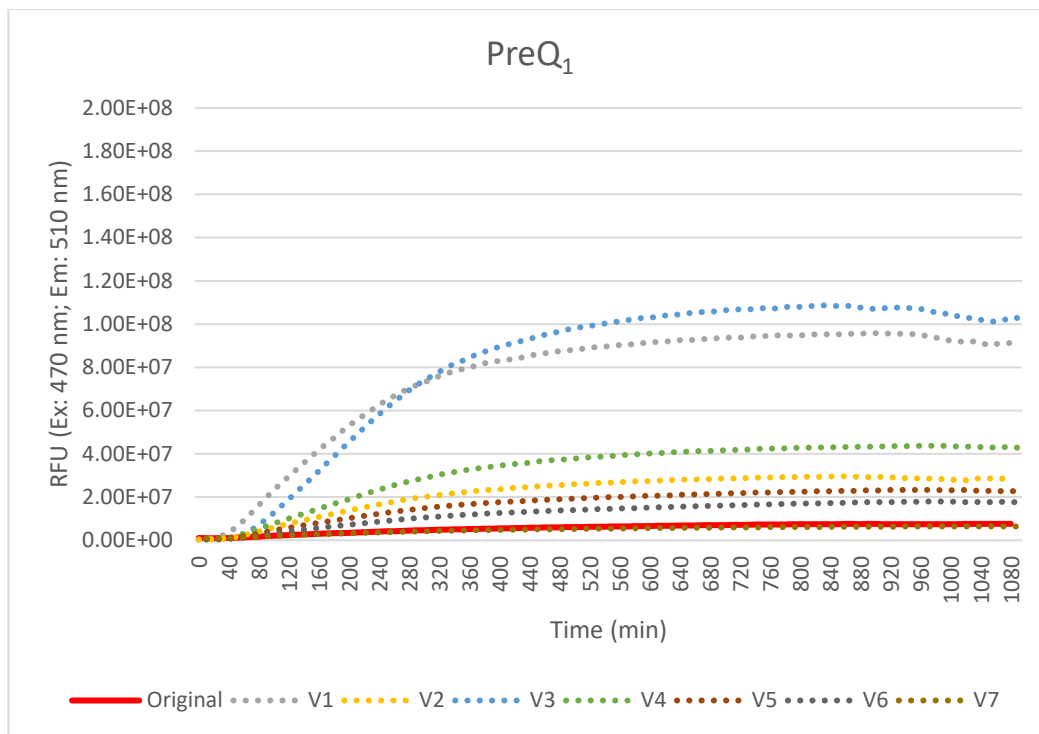
Figure 36. Riboswitch time log with PreQ$_1$
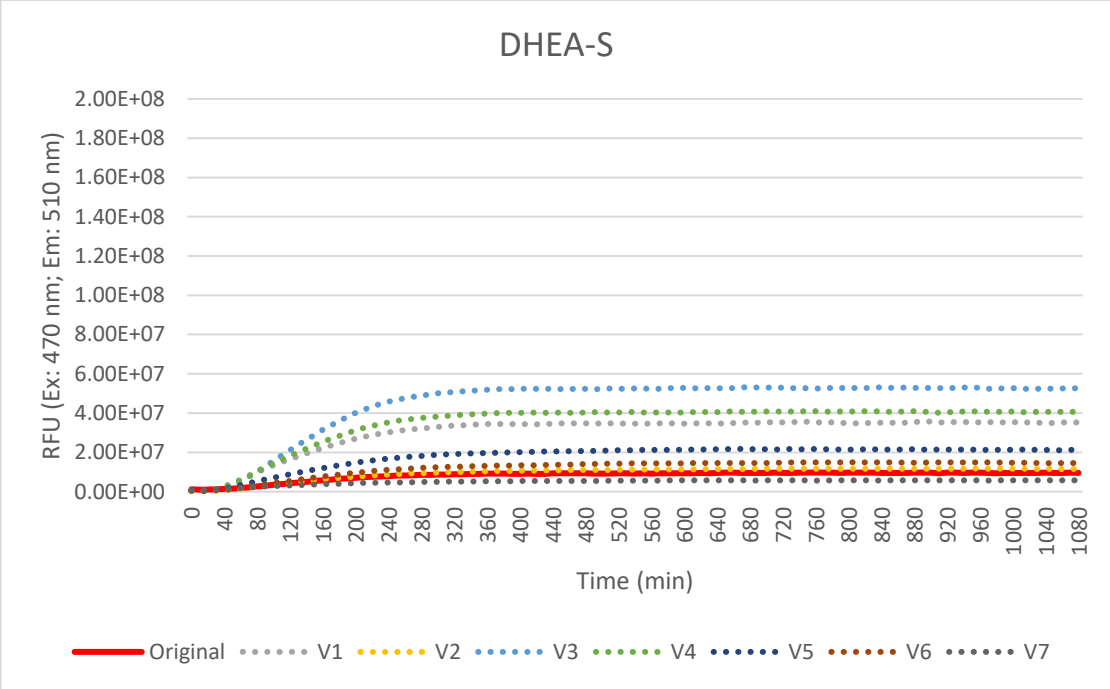
Figure 37. Riboswitch time log with DHEA-S
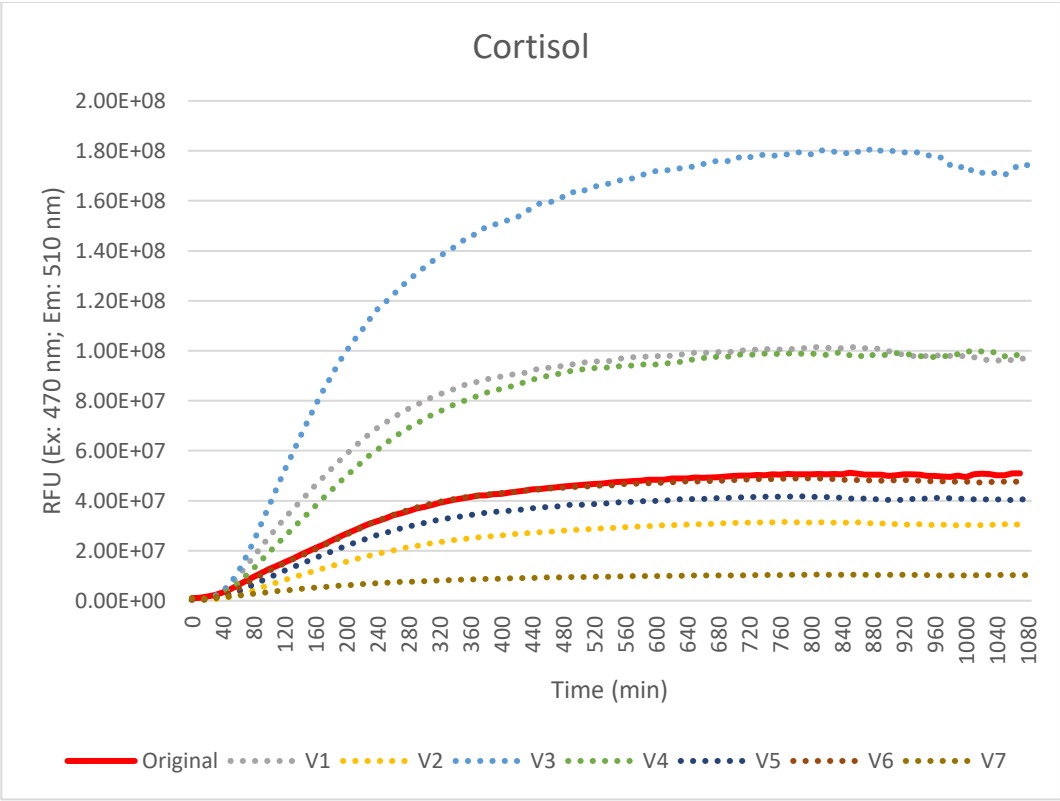
Figure 38. Riboswitch time log with Cortisol
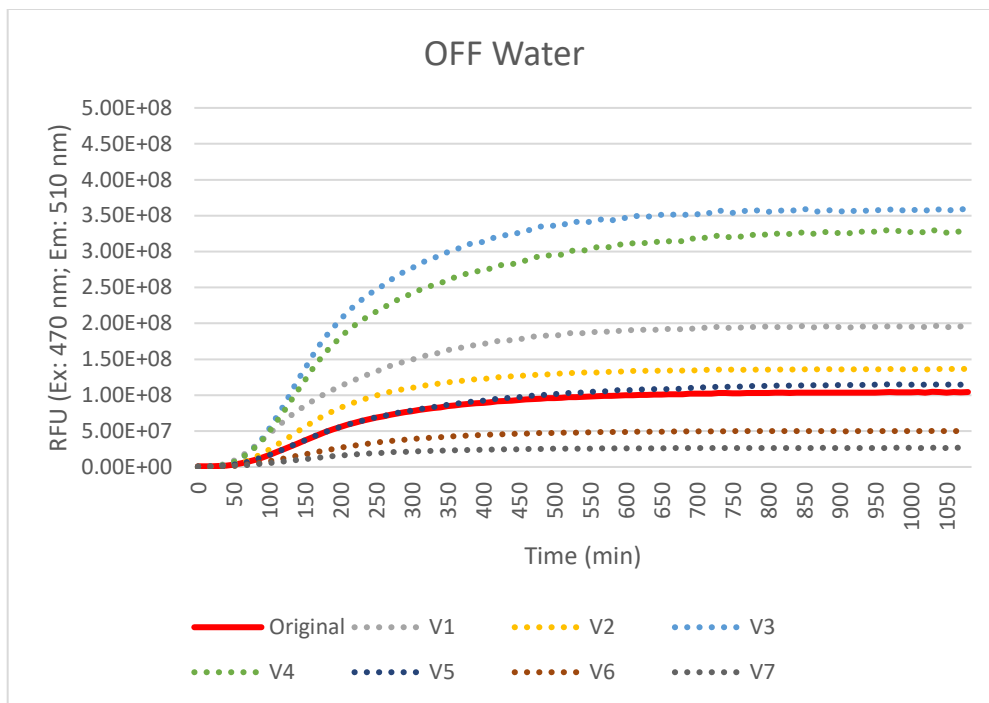
Figure 39. Riboswitch time log with OFF Water
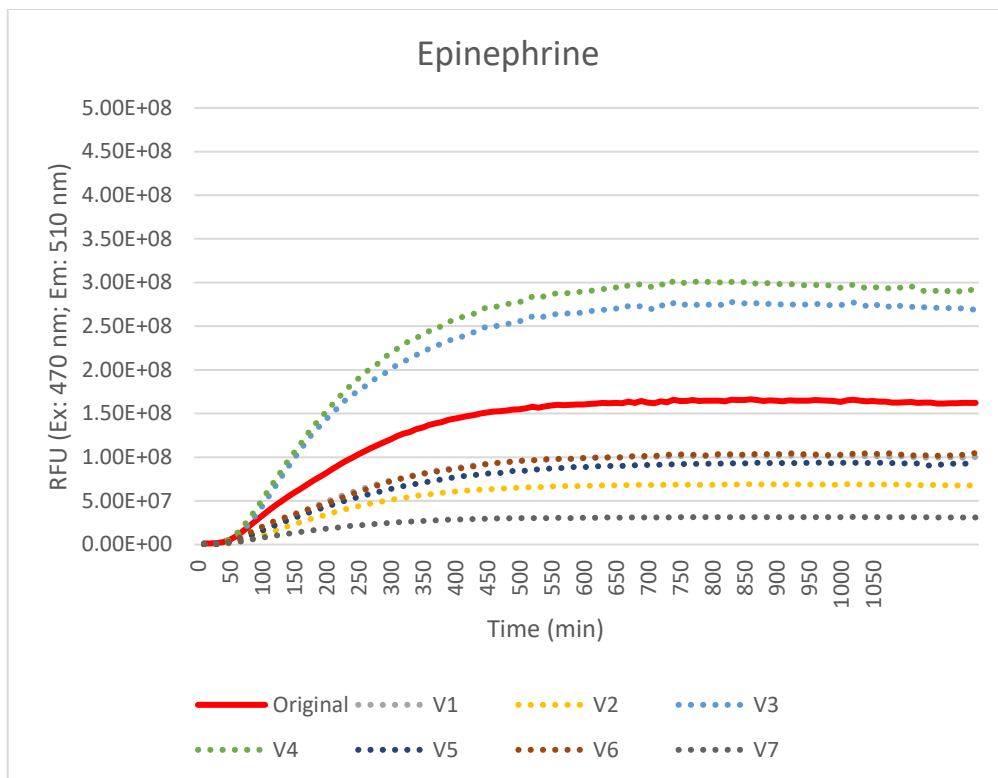
Figure 40. Riboswitch time log with Epinephrine
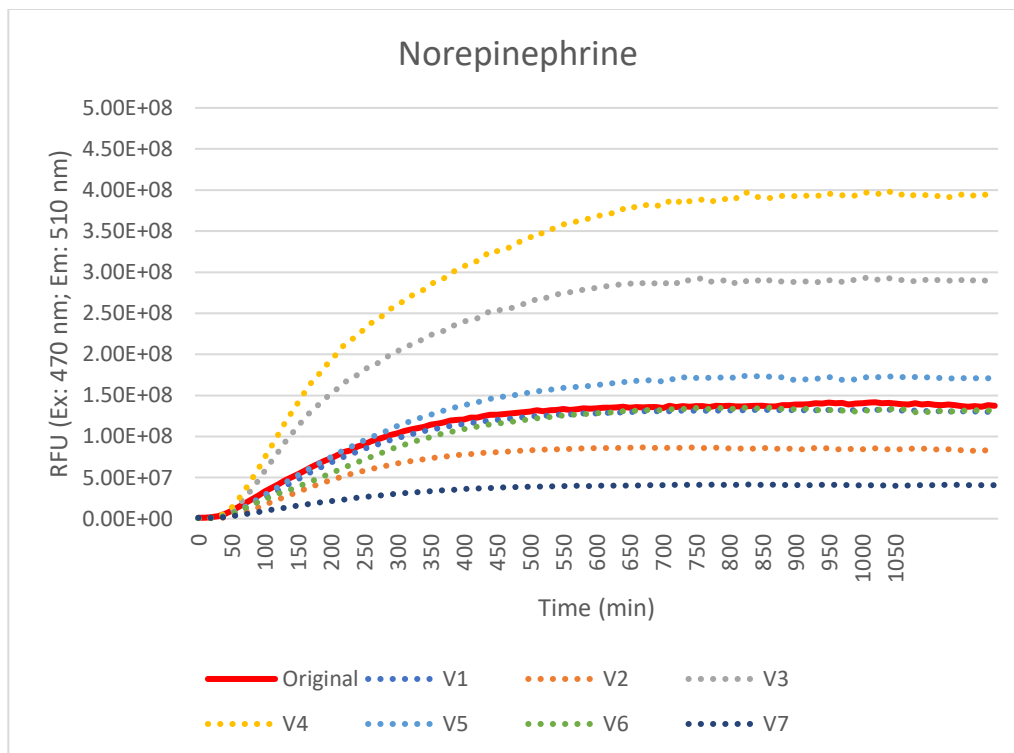
Figure 41. Riboswitch time log with Norepinephrine
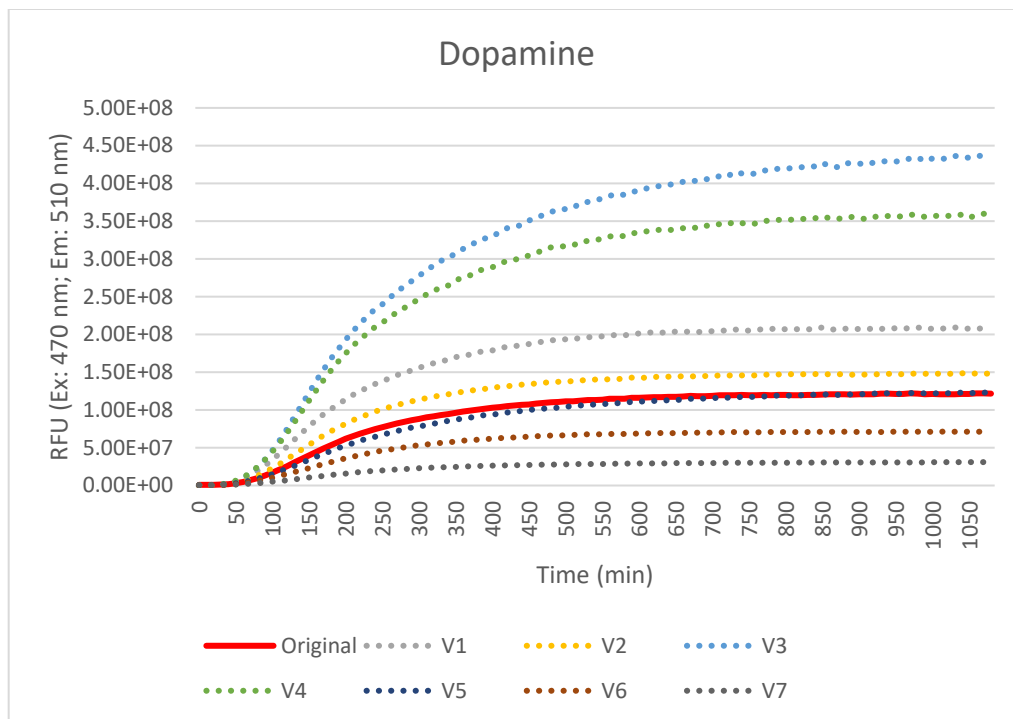
Figure 42. Riboswitch time log with Dopamine
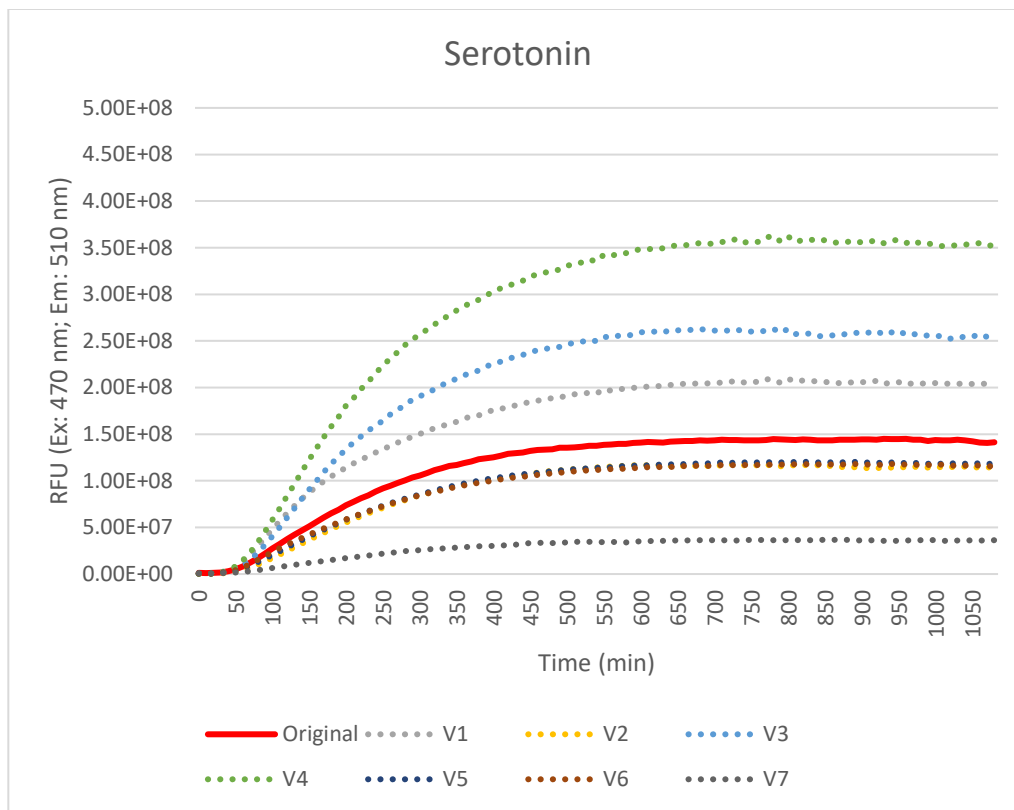
Figure 43. Riboswitch time log with Serotonin

The graphs above show the variants over time with reference to the preQ$_1$, while the date shown in Biomarker Results show the peak of each variant ON to OFF.

4.3 Biomarker Results

The following figures, Figure 44-50, show the riboswitch peak activation results from the Time Response data above. This data is extracted from the time activation graphs when the riboswitch peaks and levels off. The bar graphs are comparing PreQ$_1$ as the original riboswitch and each of the variants with the two bars showing an OFF versus ON. The difference in the bar values show how the riboswitch is transcribing or

terminated. In the figures, the orange bars will represent the OFF state and the blue bars will represent the ON state. When the riboswitch is OFF, the ligand is not attached to the aptamer, and the gene expression is on. When the riboswitch is ON, the ligand is attached to the aptamer, and the expression is terminated. This is shown from the OFF being higher than the ON. This is expected due to the gene expression being on when the aptamer is not attached to the ligand. Variants 1 and 2 do not follow this by the ON, when the ligand is bonded, being higher.
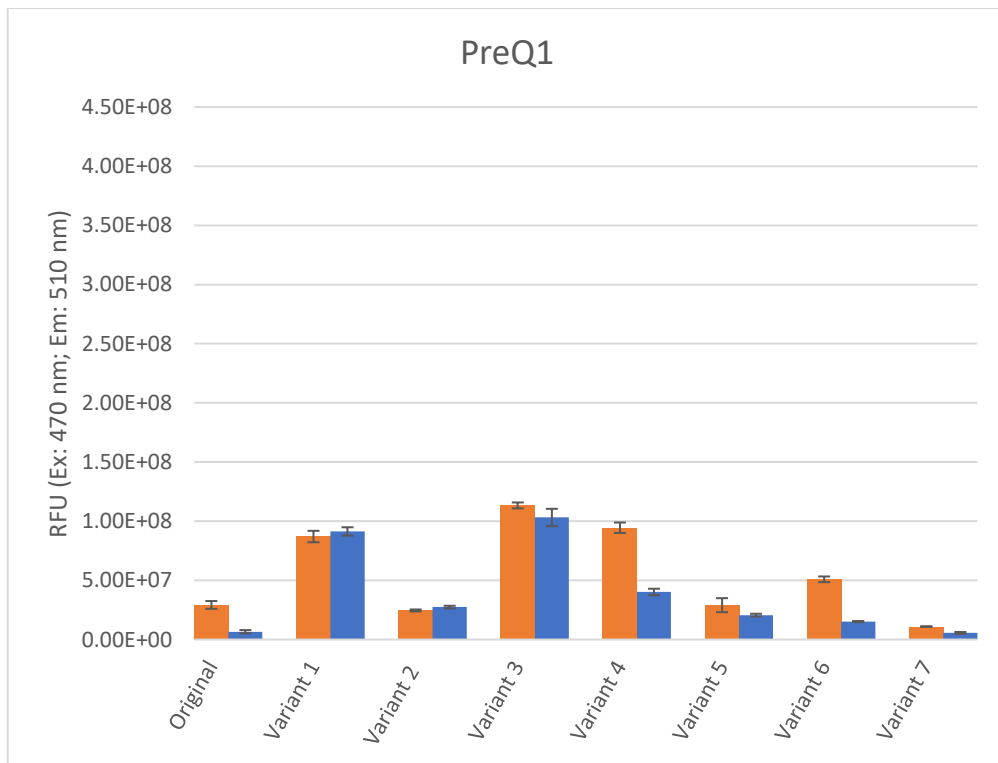
Figure 44. PreQ$_1$ biomarker against original riboswitch and variants

PreQ$_1$ is an example of how the riboswitch should respond. The following biomarkers that were tested are being compared to the original riboswitch, as well as the above

figure. DHEA-S shows a difference with how the variants all follow the original riboswitch response. Variants 1 and 2 did not follow the original response with the $preQ_1$ analyte though. Due to a different relationship with $PreQ_1$ and DHEA-S for variants 1 and 2, the Variant Response is shown to expand on this.
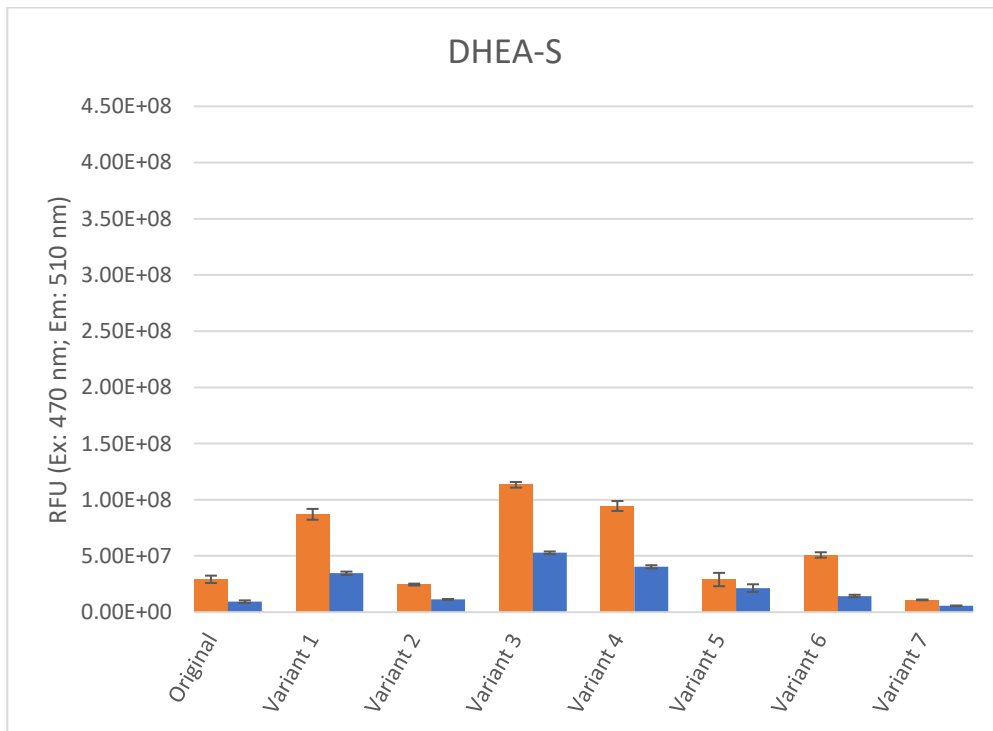
Figure 45. DHEA-S biomarker against original riboswitch and variants

The following figures differ from $preQ_1$ by the ON state being higher than the OFF state. In cases when variant 3-7 responds differently than the original, it could be due to error. This is shown in cortisol, where variant 6 is slightly higher in the OFF state than ON. The standard deviation is shown by the bars in the figures for this. This is also shown in serotonin with variant 4 and epinephrine with variants 3 and 4.
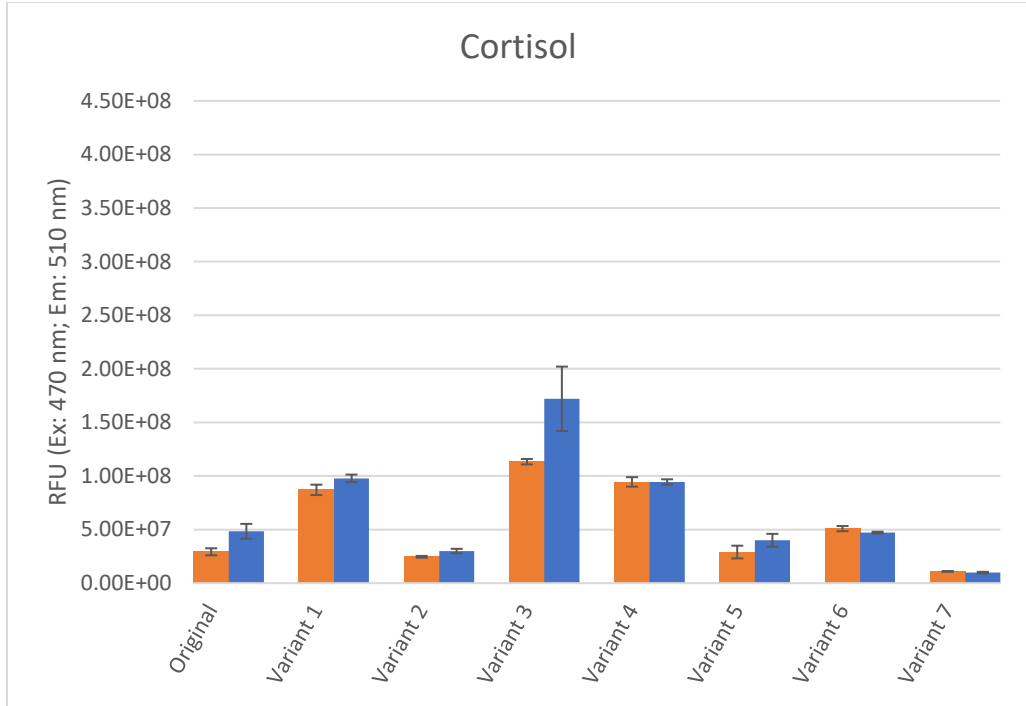
Figure 46. Cortisol biomarker against original riboswitch and variants
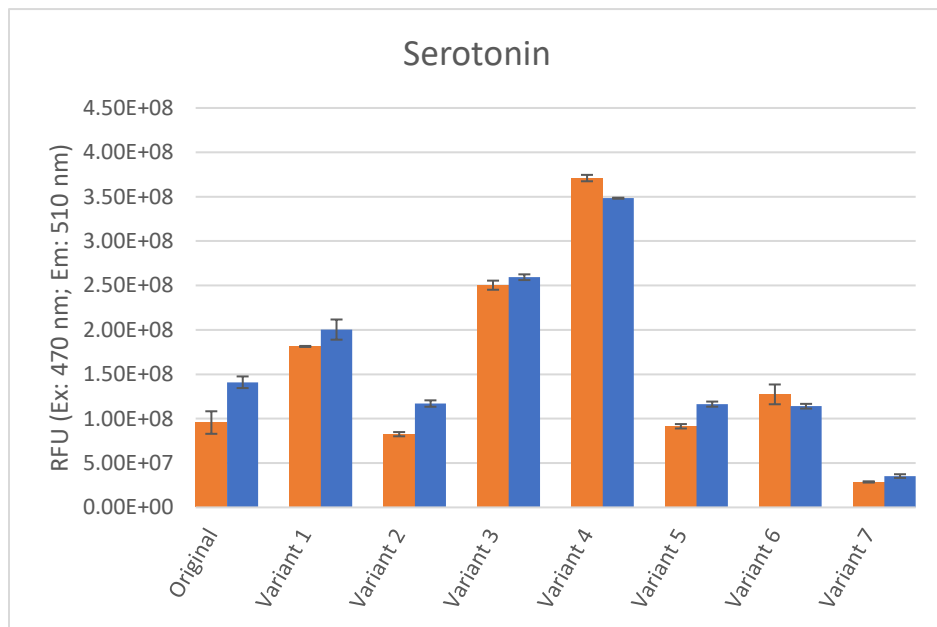
Figure 47. Serotonin biomarker against original riboswitch and variants
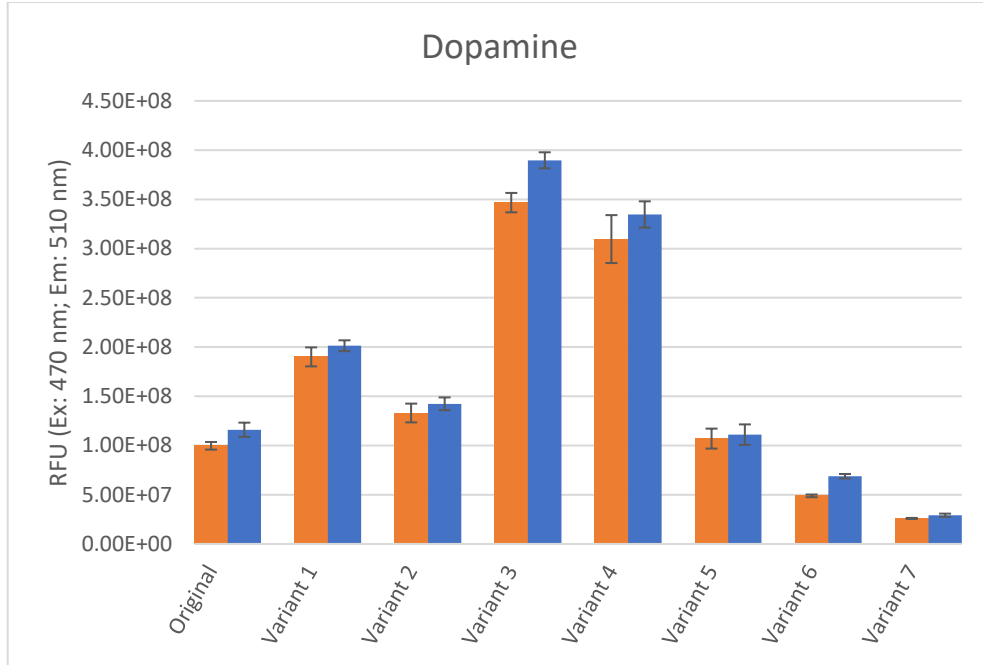
Figure 48. Dopamine biomarker against original riboswitch and variants
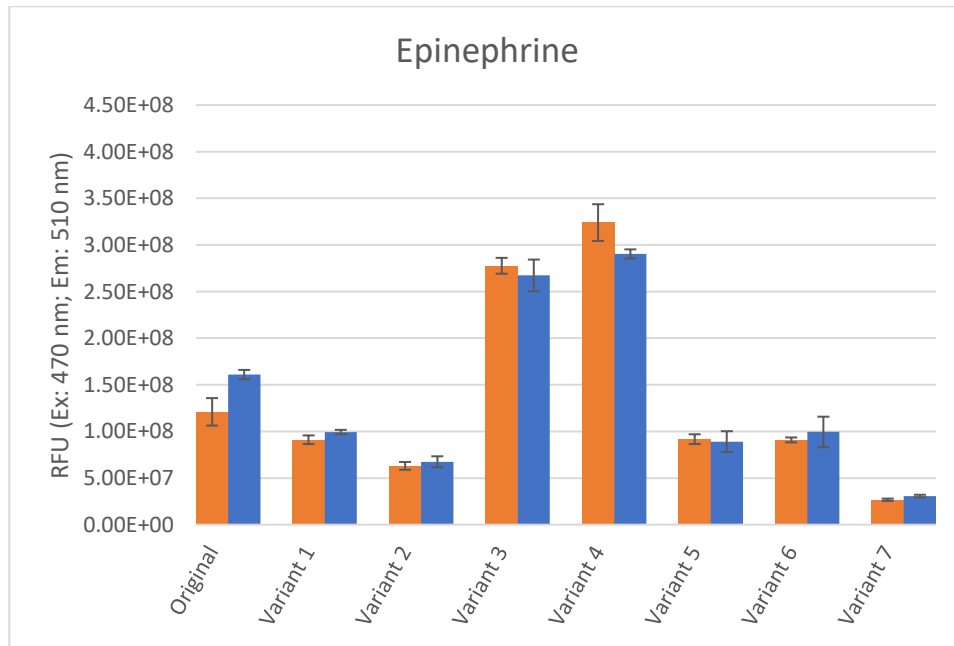
Figure 49. Epinephrine biomarker against original riboswitch and variants
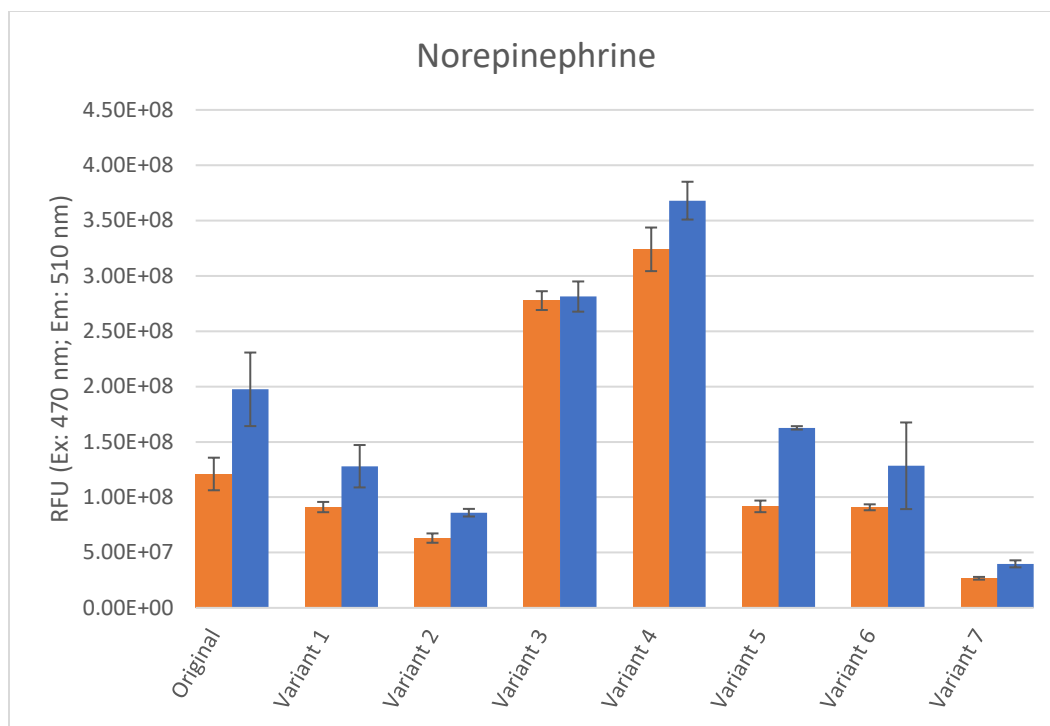
Figure 50. Norepinephrine biomarker against original riboswitch and variants

4.4 Variant Results

In this section, $PreQ_1$, Variant 1, and Variant 2 are expanded. The following figures, Figure 51-53, take the data that was presented above and show the riboswitches Original, Variant 1, and Variant 2 response with each analyte in the same figure. The bars follow the same pattern as above with orange bar is OFF, and the blue bar is ON. Variant 1 and 2 responses are compared to $PreQ_1$. The focus on this is looking at the aptamer of the riboswitch binding to the $PreQ_1$ and DHEA-S ligand. The response shows $preQ_1$ and DHEA-S respond the same with the original $PreQ_1$ riboswitch but differs in variant 1 and 2. In $PreQ_1$'s response, the relationship of OFF to ON is OFF being higher with $PreQ_1$ and DHEA-S and ON higher for all others. The difference with Variants 1 and 2 response

is that DHEA-S follows the original, but PreQ$_1$ does not. Due to this a dosage test was conducted. The results are shown below in the Dosage Results for Variants 1 and 2 section.
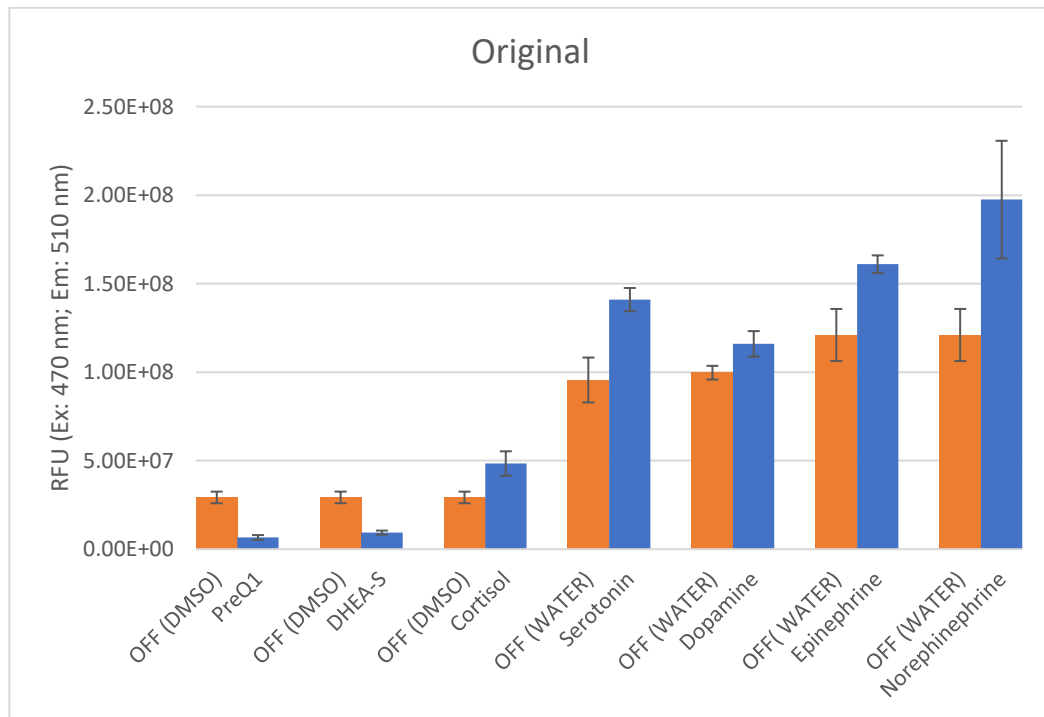
Figure 51. PreQ$_1$ riboswitch against different biomarkers
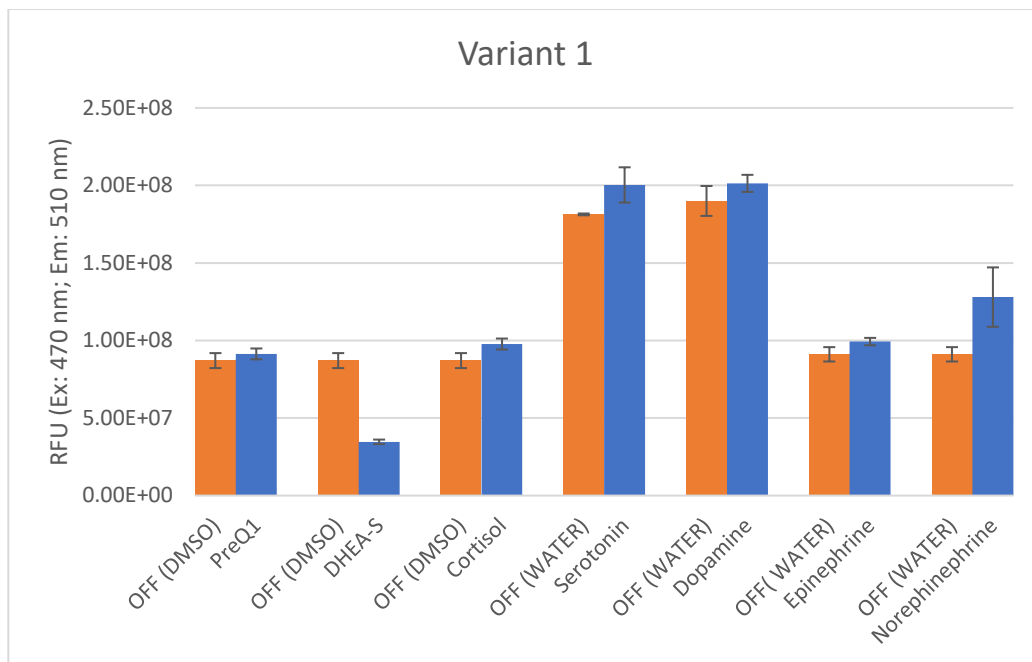
Figure 52. Variant 1 riboswitch against different biomarkers
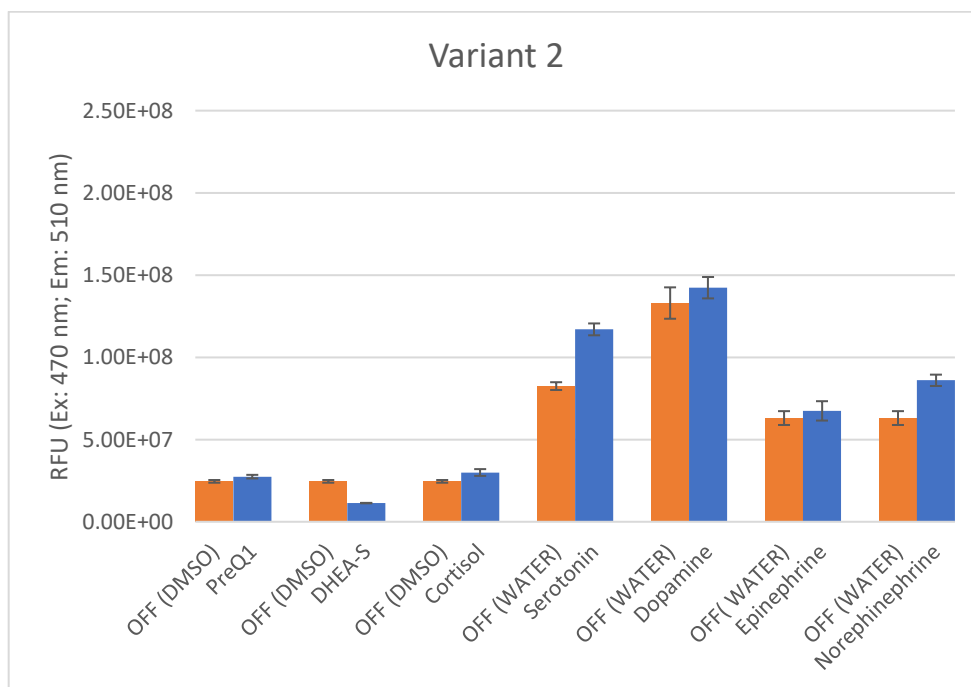
Figure 53. Variant 2 riboswitch against different biomarkers

4.5 Dosage Results for Variant 1 and 2

In this section, variants 1 and 2 are shown with different concentrations of DHEA-S. For both responses, there is a downward tread with a higher concentration of DHEA-S. The following figures, Figure 54 and 55, show variant 1 and 2 response to different concentrations of DHEA-S. The concentrations used for the dose response are concentrations found in the body.
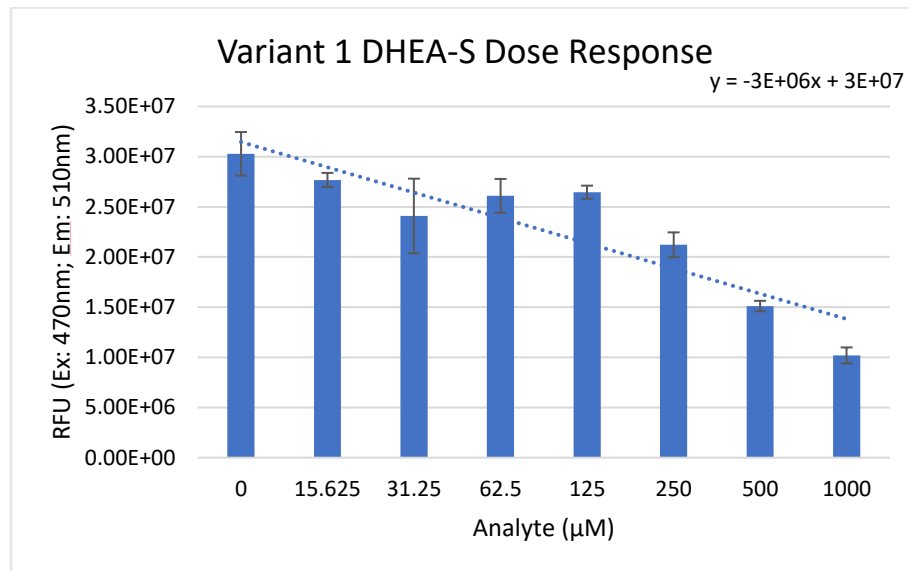
Figure 54. Variant 1 against DHEA-S Dose Response
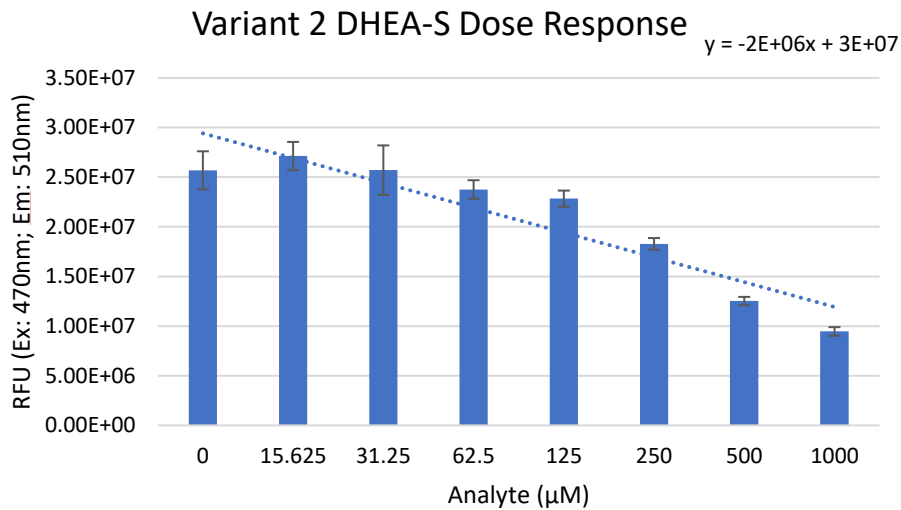
Figure 55. Variant 2 against DHEA-S Dose Response

In the above figures, Figure 54 and 55, the drug response may be described by a linear fit.

Drug dose and response is mathematically represented in terms of a sigmoidal function.

Such function allows generation of a S curve that plots the behavior from a lower point

(usually negative to positive) to higher. Thus, the S curve. Since the physiologic behavior

represents only the positive concentration, studied in this paper, the dose characteristics

are described by a linear equation as the figure shows. Each on the trendline fit shows a

negative slope.1

As it shows on Figure 54 and 55, the equations have a negative linear trend. This is due to

the riboswitch having a higher RFU since there is no DHEA-S and the riboswitch being

OFF and transcribing proteins. Comparing these graphs to the time activation graphs and

biomarker graphs for DHEA-S and PreQ$_1$, the trendlines follow the same pattern. As the

concentration of the analyte increases, the variants are showing how they terminated their

protein production. If this was $PreQ_1$ as the analyte, the production would stay the same as the concentration increases.

5. CONCLUSION

This research describes the methods of reengineering riboswitches. In this experimentation, $PreQ_1$ was examined and engineered into four new variants. Through the computational and experimental procedures that were conducted, it is shown that two of these variants responded to DHEA-S differently than $PreQ_1$. From reference research, three variants were tested with the same procedures and showed no new data. In conclusion, it can be confirmed that riboswitches can be reengineered to respond to different biomarkers.

Based on the presented data analysis above, it can be concluded that variants 1 and 2 were reengineered to respond to DHEA-S when the original riboswitch did not. The computational data confirms this through variants 1 and 2 having equilibrium probabilities that indicate the structural formation would not be likely. Variants 3 and 4 indicated to show results similar to $PreQ_1$ based on their equilibrium probability. This is also shown through the response of variants 1 and 2 differing when testing against $PreQ_1$. All variants had similar results when presented with the aptamer $PreQ_1$. This change did not affect the response against DHEA-S though. Due to this, a closer examination was done through a dose response test. This test confirmed this conclusion, by having a downward tread as the concentrations of DHEA-S increased.

Continuing this research can be done by looking at different biomarkers with the variants that were used in this research. The riboswitch, $PreQ_1$, can also be reengineered with different variants. Along with those suggestions, the designing by computer

software's can be used with part research to help confirm variant riboswitches that were based off known riboswitches.

6. REFERENCES

[1] B. M. Brandsen, J. M. Mattheisen, T. Noel, and S. Fields, "A Biosensor Strategy for *E. coli* Based on Ligand-Dependent Stabilization," *ACS Synth. Biol.*, vol. 7, no. 9, pp. 1990–1999, Sep. 2018, doi: 10.1021/acssynbio.8b00052.

[2] A. Serganov and E. Nudler, "A Decade of Riboswitches," *Cell*, vol. 152, no. 1–2, pp. 17–24, Jan. 2013, doi: 10.1016/j.cell.2012.12.024.

[3] G. Zhong *et al.*, "A reversible RNA on-switch that controls gene expression of AAV-delivered therapeutics in vivo," *Nat. Biotechnol.*, vol. 38, no. 2, pp. 169–175, Feb. 2020, doi: 10.1038/s41587-019-0357-y.

[4] M. Zhang, F. Zhou, D. Zhou, D. Chen, H. Hai, and J. Li, "An aptamer biosensor for leukemia marker mRNA detection based on polymerase-assisted signal amplification and aggregation of illuminator," *Anal. Bioanal. Chem.*, vol. 411, no. 1, pp. 139–146, Jan. 2019, doi: 10.1007/s00216-018-1424-9.

[5] M. Kirchner, K. Schorpp, K. Hadian, and S. Schneider, "An in vivo high-throughput screening for riboswitch ligands using a reverse reporter gene system," *Sci. Rep.*, vol. 7, Aug. 2017, doi: 10.1038/s41598-017-07870-w.

[6] J. Noeske, C. Richter, M. A. Grundl, H. R. Nasiri, H. Schwalbe, and J. Wohnert, "An intermolecular base triple as the basis of ligand specificity and affinity in the guanine- and adenine-sensing riboswitch RNAs," *Proc. Natl. Acad. Sci.*, vol. 102, no. 5, pp. 1372–1377, Feb. 2005, doi: 10.1073/pnas.0406347102.

[7] N. Sudarsan, "An mRNA structure in bacteria that controls gene expression by binding lysine," *Genes Dev.*, vol. 17, no. 21, pp. 2688–2697, Oct. 2003, doi: 10.1101/gad.1140003.

[8] J. K. Michener, K. Thodey, J. C. Liang, and C. D. Smolke, "Applications of genetically-encoded biosensors for the construction and control of biosynthetic pathways," *Metab. Eng.*, vol. 14, no. 3, pp. 212–222, May 2012, doi: 10.1016/j.ymben.2011.09.004.

[9] J. Cruz-Toledo *et al.*, "Aptamer base: a collaborative knowledge base to describe aptamers and SELEX experiments," *Database*, vol. 2012, Jan. 2012, doi: 10.1093/database/bas006.

[10] Y. Yokobayashi, "Aptamer-based and aptazyme-based riboswitches in mammalian cells," *Curr. Opin. Chem. Biol.*, vol. 52, pp. 72–78, Oct. 2019, doi: 10.1016/j.cbpa.2019.05.018.

[11] A. Joergensen *et al.*, "Association between Urinary Excretion of Cortisol and Markers of Oxidatively Damaged DNA and RNA in Humans," *PLoS ONE*, vol. 6, no. 6, p. e20795, Jun. 2011, doi: 10.1371/journal.pone.0020795.

[12] A. Espah Borujeni, D. M. Mishler, J. Wang, W. Huso, and H. M. Salis, "Automated physics-based design of synthetic riboswitches from diverse RNA aptamers," *Nucleic Acids Res.*, vol. 44, no. 1, pp. 1–13, Jan. 2016, doi: 10.1093/nar/gkv1289.

[13] J. E. Johnson, F. E. Reyes, J. T. Polaski, and R. T. Batey, "B12 cofactors directly stabilize an mRNA regulatory switch," *Nature*, vol. 492, no. 7427, pp. 133–137, Dec. 2012, doi: 10.1038/nature11607.

[14] S. Rachid Zaim *et al.*, "binomialRF: interpretable combinatoric efficiency of random forests to identify biomarker interactions," *BMC Bioinformatics*, vol. 21, no. 1, p. 374, Dec. 2020, doi: 10.1186/s12859-020-03718-9.

[15] Z. Weinberg, J. W. Nelson, C. E. Lünse, M. E. Sherlock, and R. R. Breaker, "Bioinformatic analysis of riboswitch structures uncovers variant classes with altered ligand specificity," *Proc. Natl. Acad. Sci.*, vol. 114, no. 11, pp. E2077–E2085, Mar. 2017, doi: 10.1073/pnas.1619581114.

[16] M. González-Gross, "Biomarcadores de la actividad física y del deporte," *Nutr. Hosp.*, no. 3, pp. 237–244, Feb. 2015, doi: 10.3305/nh.2015.31.sup3.8771.

[17] C. Young, R. Sharma, M. Handfield, V. Mai, and J. Neu, "Biomarkers for Infants at Risk for Necrotizing Enterocolitis: Clues to Prevention?," *Pediatr. Res.*, vol. 65, no. 5 Part 2, pp. 91R-97R, May 2009, doi: 10.1203/PDR.0b013e31819dba7d.

[18] E. C. Lee, M. S. Fragala, S. A. Kavouras, R. M. Queen, J. L. Pryor, and D. J. Casa, "Biomarkers in Sports and Exercise: Tracking Health, Performance, and Recovery in Athletes," *J. Strength Cond. Res.*, vol. 31, no. 10, pp. 2920–2937, Oct. 2017, doi: 10.1519/JSC.0000000000002122.

[19] R. Mayeux, "Biomarkers: Potential Uses and Limitations," *NeuroRx*, vol. 1, no. 2, pp. 182–188, Apr. 2004.

[20] F. Perroni *et al.*, "Can Haematological and Hormonal Biomarkers Predict Fitness Parameters in Youth Soccer Players? A Pilot Study," *Int. J. Environ. Res. Public. Health*, vol. 17, no. 17, p. 6294, Aug. 2020, doi: 10.3390/ijerph17176294.

[21] K. Suzuki, "Chronic Inflammation as an Immunological Abnormality and Effectiveness of Exercise," *Biomolecules*, vol. 9, no. 6, Jun. 2019, doi: 10.3390/biom9060223.

[22] J.-F. Lemay *et al.*, "Comparative Study between Transcriptionally- and Translationally-Acting Adenine Riboswitches Reveals Key Differences in Riboswitch Regulatory Mechanisms," *PLoS Genet.*, vol. 7, no. 1, Jan. 2011, doi: 10.1371/journal.pgen.1001278.

[23] J. L. Jenkins, J. Krucinska, R. M. McCarty, V. Bandarian, and J. E. Wedekind, "Comparison of a PreQ1 Riboswitch Aptamer in Metabolite-bound and Free States with Implications for Gene Regulation," *J. Biol. Chem.*, vol. 286, no. 28, pp. 24626–24637, Jul. 2011, doi: 10.1074/jbc.M111.230375.

[24] E. I. Sun and D. A. Rodionov, "Computational analysis of riboswitch-based regulation," *Biochim. Biophys. Acta BBA - Gene Regul. Mech.*, vol. 1839, no. 10, pp. 900–907, Oct. 2014, doi: 10.1016/j.bbagrm.2014.02.011.

[25] L. L. Smith, "Cytokine hypothesis of overtraining: a physiological adaptation to excessive stress?:," *Med. Sci. Sports Exerc.*, vol. 32, no. 2, p. 317, Feb. 2000, doi: 10.1097/00005768-200002000-00011.

[26] K. J. de Menezes, C. Peixoto, A. E. Nardi, M. G. Carta, S. Machado, and A. B. Veras, "Dehydroepiandrosterone, Its Sulfate and Cognitive Functions," *Clin. Pract. Epidemiol. Ment. Health*, vol. 12, no. 1, pp. 24–37, Apr. 2016, doi: 10.2174/1745017901612010024.

[27] S. Findeiß, M. Etzel, S. Will, M. Mörl, and P. Stadler, "Design of Artificial Riboswitches as Biosensors," *Sensors*, vol. 17, no. 9, p. 1990, Aug. 2017, doi: 10.3390/s17091990.

[28] K. Mustafina, K. Fukunaga, and Y. Yokobayashi, "Design of Mammalian ON-Riboswitches Based on Tandemly Fused Aptamer and Ribozyme," *ACS Synth. Biol.*, vol. 9, no. 1, pp. 19–25, Jan. 2020, doi: 10.1021/acssynbio.9b00371.

[29] J. J. Trausch and R. T. Batey, "Design of Modular 'Plug-and-Play' Expression Platforms Derived from Natural Riboswitches for Engineering Novel Genetically Encodable RNA Regulatory Devices," in *Methods in Enzymology*, vol. 550, Elsevier, 2015, pp. 41–71. doi: 10.1016/bs.mie.2014.10.031.

[30] M. O. Klein, D. S. Battagello, A. R. Cardoso, D. N. Hauser, J. C. Bittencourt, and R. G. Correa, "Dopamine: Functions, Signaling, and Association with Neurological Diseases," *Cell. Mol. Neurobiol.*, vol. 39, no. 1, pp. 31–59, Jan. 2019, doi: 10.1007/s10571-018-0632-3.

[31] R. R. Breaker, "Engineered allosteric ribozymes as biosensor components," *Curr. Opin. Biotechnol.*, vol. 13, no. 1, pp. 31–39, Feb. 2002, doi: 10.1016/S0958-1669(02)00281-1.

[32] S. Ketterer, L. Gladis, A. Kozica, and M. Meier, "Engineering and characterization of fluorogenic glycine riboswitches," *Nucleic Acids Res.*, vol. 44, no. 12, pp. 5983–5992, Jul. 2016, doi: 10.1093/nar/gkw465.

[33] R. Galizi and A. Jaramillo, "Engineering CRISPR guide RNA riboswitches for in vivo applications," *Curr. Opin. Biotechnol.*, vol. 55, pp. 103–113, Feb. 2019, doi: 10.1016/j.copbio.2018.08.007.

[34] P. Ceres, J. J. Trausch, and R. T. Batey, "Engineering modular 'ON' RNA switches using biological components," *Nucleic Acids Res.*, vol. 41, no. 22, pp. 10449–10461, Dec. 2013, doi: 10.1093/nar/gkt787.

[35] K. Page, J. Shaffer, S. Lin, M. Zhang, and J. M. Liu, "Engineering Riboswitches *in Vivo* Using Dual Genetic Selection and Fluorescence-Activated Cell Sorting," *ACS Synth. Biol.*, vol. 7, no. 9, pp. 2000–2006, Sep. 2018, doi: 10.1021/acssynbio.8b00099.

[36] S. Li and R. R. Breaker, "Eukaryotic TPP riboswitch regulation of alternative splicing involving long-distance base pairing," *Nucleic Acids Res.*, vol. 41, no. 5, pp. 3022–3031, Mar. 2013, doi: 10.1093/nar/gkt057.

[37] D. da L. Scheffer and A. Latini, "Exercise-induced immune system response: Anti-inflammatory status on peripheral and central organs," *Biochim. Biophys. Acta BBA - Mol. Basis Dis.*, vol. 1866, no. 10, p. 165823, Oct. 2020, doi: 10.1016/j.bbadis.2020.165823.

[38] L. Yang, J. Li, W. Pan, H. Wang, N. Li, and B. Tang, "Fluorescence and photoacoustic dual-mode imaging of tumor-related mRNA with a covalent linkage-based DNA nanoprobe," *Chem. Commun.*, vol. 54, no. 29, pp. 3656–3659, 2018, doi: 10.1039/C8CC01335G.

[39] A. Haller, R. B. Altman, M. F. Soulière, S. C. Blanchard, and R. Micura, "Folding and ligand recognition of the TPP riboswitch aptamer at single-molecule resolution," *Proc. Natl. Acad. Sci.*, vol. 110, no. 11, pp. 4188–4193, Mar. 2013, doi: 10.1073/pnas.1218062110.

[40] P. C. Anthony, C. F. Perez, C. Garcia-Garcia, and S. M. Block, "Folding energy landscape of the thiamine pyrophosphate riboswitch aptamer," *Proc. Natl. Acad. Sci.*, vol. 109, no. 5, pp. 1485–1489, Jan. 2012, doi: 10.1073/pnas.1115045109.

[41] M. E. Sherlock and R. R. Breaker, "Former orphan riboswitches reveal unexplored areas of bacterial metabolism, signaling, and gene control processes," *RNA*, vol. 26, no. 6, pp. 675–693, Jun. 2020, doi: 10.1261/rna.074997.120.

[42] M. K. Cabaj and P. M. Dominiak, "Frequency and hydrogen bonding of nucleobase homopairs in small molecule crystals," *Nucleic Acids Res.*, vol. 48, no. 15, pp. 8302–8319, Sep. 2020, doi: 10.1093/nar/gkaa629.

[43] J. N. Kim, A. Roth, and R. R. Breaker, "Guanine riboswitch variants from Mesoplasma florum selectively recognize 2′-deoxyguanosine," *Proc. Natl. Acad. Sci. U. S. A.*, vol. 104, no. 41, pp. 16092–16097, Oct. 2007, doi: 10.1073/pnas.0705884104.

[44] A. Subki, C. L. Ho, N. F. N. Ismail, A. A. Zainal Abidin, and Z. N. Balia Yusof,
"Identification and characterisation of thiamine pyrophosphate (TPP) riboswitch in
Elaeis guineensis," *PLOS ONE*, vol. 15, no. 7, p. e0235431, Jul. 2020, doi:
10.1371/journal.pone.0235431.

[45] C. Schneider and B. Suess, "Identification of RNA aptamers with riboswitching
properties," *Methods*, vol. 97, pp. 44–50, Mar. 2016, doi:
10.1016/j.ymeth.2015.12.001.

[46] Z. Gong, Y. Zhao, C. Chen, Y. Duan, and Y. Xiao, "Insights into Ligand Binding to
PreQ1 Riboswitch Aptamer from Molecular Dynamics Simulations," *PLoS ONE*,
vol. 9, no. 3, p. e92247, Mar. 2014, doi: 10.1371/journal.pone.0092247.

[47] B. K. Pedersen and M. A. Febbraio, "Interleukin-6 does/does not have a beneficial
role in insulin sensitivity and glucose homeostasis," *J. Appl. Physiol.*, vol. 102, no.
2, pp. 814–816, Feb. 2007, doi: 10.1152/japplphysiol.01208.2006.

[48] N. Segata *et al.*, "Metagenomic biomarker discovery and explanation," *Genome
Biol.*, vol. 12, no. 6, p. R60, 2011, doi: 10.1186/gb-2011-12-6-r60.

[49] C. Banerjee, P. K. Singh, and P. Shukla, "Microalgal bioengineering for sustainable
energy development: Recent transgenesis and metabolic engineering strategies,"
Biotechnol. J., vol. 11, no. 3, pp. 303–314, Mar. 2016, doi: 10.1002/biot.201500284.

[50] W. Thavarajah, A. D. Silverman, M. S. Verosloff, N. Kelley-Loughnane, M. C.
Jewett, and J. B. Lucks, "Point-of-Use Detection of Environmental Fluoride *via* a

Cell-Free Riboswitch-Based Biosensor," *ACS Synth. Biol.*, vol. 9, no. 1, pp. 10–18, Jan. 2020, doi: 10.1021/acssynbio.9b00347.

[51] R. R. Breaker, "Prospects for Riboswitch Discovery and Analysis," *Mol. Cell*, vol. 43, no. 6, pp. 867–879, Sep. 2011, doi: 10.1016/j.molcel.2011.08.024.

[52] S. Guedich *et al.*, "Quantitative and predictive model of kinetic regulation by E. coli TPP riboswitches," *RNA Biol.*, vol. 13, no. 4, pp. 373–390, Apr. 2016, doi: 10.1080/15476286.2016.1142040.

[53] M.-C. Wu *et al.*, "Rational Re-engineering of a Transcriptional Silencing PreQ $_1$ Riboswitch," *J. Am. Chem. Soc.*, vol. 137, no. 28, pp. 9015–9021, Jul. 2015, doi: 10.1021/jacs.5b03405.

[54] Y. Nomura and Y. Yokobayashi, "Reengineering a Natural Riboswitch by Dual Genetic Selection," *J. Am. Chem. Soc.*, vol. 129, no. 45, pp. 13814–13815, Nov. 2007, doi: 10.1021/ja076298b.

[55] S. Capellino, M. Claus, and C. Watzl, "Regulation of natural killer cell activity by glucocorticoids, serotonin, dopamine, and epinephrine," *Cell. Mol. Immunol.*, vol. 17, no. 7, pp. 705–711, Jul. 2020, doi: 10.1038/s41423-020-0477-9.

[56] C. E. Lünse and G. Mayer, "Reporter Gene-Based Screening for TPP Riboswitch Activators," in *Antibiotics*, vol. 1520, P. Sass, Ed. New York, NY: Springer New York, 2017, pp. 227–235. doi: 10.1007/978-1-4939-6634-9_13.

[57] L. K. Drogalis and R. T. Batey, "Requirements for efficient cotranscriptional regulatory switching in designed variants of the *Bacillus subtilis pbuE* adenine-responsive riboswitch," Biochemistry, preprint, Jul. 2018. doi: 10.1101/372573.

[58] N. Pavlova, D. Kaloudas, and R. Penchovsky, "Riboswitch distribution, structure, and function in bacteria," *Gene*, vol. 708, pp. 38–48, Aug. 2019, doi: 10.1016/j.gene.2019.05.036.

[59] C. Berens and B. Suess, "Riboswitch engineering — making the all-important second and third steps," *Curr. Opin. Biotechnol.*, vol. 31, pp. 10–15, Feb. 2015, doi: 10.1016/j.copbio.2014.07.014.

[60] J. A. Liberman and J. E. Wedekind, "Riboswitch structure in the ligand-free state: Riboswitch structure in the ligand-free state," *Wiley Interdiscip. Rev. RNA*, vol. 3, no. 3, pp. 369–384, May 2012, doi: 10.1002/wrna.114.

[61] R. R. Breaker, "Riboswitches and the RNA World," *Cold Spring Harb. Perspect. Biol.*, vol. 4, no. 2, pp. a003566–a003566, Feb. 2012, doi: 10.1101/cshperspect.a003566.

[62] "Riboswitches, RNA Regulation | Learn Science at Scitable." https://www.nature.com/scitable/topicpage/riboswitches-a-common-rna-regulatory-element-14262702/ (accessed Dec. 07, 2020).

[63] J. Zhang, M. W. Lau, and A. R. Ferré-D'Amaré, "Ribozymes and Riboswitches: Modulation of RNA Function by Small Molecules," *Biochemistry*, vol. 49, no. 43, pp. 9123–9131, Nov. 2010, doi: 10.1021/bi1012645.

[64] F. Zhao, Q. Xie, M. Xu, S. Wang, J. Zhou, and F. Liu, "RNA aptamer based electrochemical biosensor for sensitive and selective detection of cAMP," *Biosens. Bioelectron.*, vol. 66, pp. 238–243, Apr. 2015, doi: 10.1016/j.bios.2014.11.024.

[65] S. Tian and R. Das, "RNA structure through multidimensional chemical mapping," *Q. Rev. Biophys.*, vol. 49, p. e7, 2016, doi: 10.1017/S0033583516000020.

[66] D. H. Hellhammer, S. Wüst, and B. M. Kudielka, "Salivary cortisol as a biomarker in stress research," *Psychoneuroendocrinology*, vol. 34, no. 2, pp. 163–171, Feb. 2009, doi: 10.1016/j.psyneuen.2008.10.026.

[67] D. P. Morse, C. E. Nevins, J. Aggrey-Fynn, R. J. Bravo, H. O. I. Pfaeffle, and J. E. Laney, "Sensitive and specific detection of ligands using engineered riboswitches," *J. Biotechnol.*, vol. 272–273, pp. 22–32, Apr. 2018, doi: 10.1016/j.jbiotec.2018.03.002.

[68] Z. Kang *et al.*, "Small RNA regulators in bacteria: powerful tools for metabolic engineering and synthetic biology," *Appl. Microbiol. Biotechnol.*, vol. 98, no. 8, pp. 3413–3424, Apr. 2014, doi: 10.1007/s00253-014-5569-y.

[69] A. J. Steckl and P. Ray, "Stress Biomarkers in Biological Fluids and Their Point-of-Use Detection," *ACS Sens.*, vol. 3, no. 10, pp. 2025–2044, Oct. 2018, doi: 10.1021/acssensors.8b00726.

[70] A. Serganov, A. Polonskaia, A. T. Phan, R. R. Breaker, and D. J. Patel, "Structural basis for gene regulation by a thiamine pyrophosphate-sensing riboswitch," *Nature*, vol. 441, no. 7097, Art. no. 7097, Jun. 2006, doi: 10.1038/nature04740.

[71] V. Berk, W. Zhang, R. D. Pai, and J. H. D. Cate, "Structural basis for mRNA and tRNA positioning on the ribosome," *Proc. Natl. Acad. Sci. U. S. A.*, vol. 103, no. 43, pp. 15830–15834, Oct. 2006, doi: 10.1073/pnas.0607541103.

[72] C. M. Connelly *et al.*, "Synthetic ligands for PreQ1 riboswitches provide structural and mechanistic insights into targeting RNA tertiary structure," *Nat. Commun.*, vol. 10, no. 1, p. 1501, Dec. 2019, doi: 10.1038/s41467-019-09493-3.

[73] S. Ausländer and M. Fussenegger, "Synthetic RNA-based switches for mammalian gene expression control," *Curr. Opin. Biotechnol.*, vol. 48, pp. 54–60, Dec. 2017, doi: 10.1016/j.copbio.2017.03.011.

[74] R. Schiess, B. Wollscheid, and R. Aebersold, "Targeted proteomic strategy for clinical biomarker discovery," *Mol. Oncol.*, vol. 3, no. 1, pp. 33–44, Feb. 2009, doi: 10.1016/j.molonc.2008.12.001.

[75] M. F. Schaffer, P. K. Choudhary, and R. K. O. Sigel, "The AdoCbl–Riboswitch Interaction Investigated by In-Line Probing and Surface Plasmon Resonance Spectroscopy (SPR)," in *Methods in Enzymology*, vol. 549, Elsevier, 2014, pp. 467–488. doi: 10.1016/B978-0-12-801122-5.00020-9.

[76] S. E. Harding, G. Channell, and M. K. Phillips-Jones, "The discovery of hydrogen bonds in DNA and a re-evaluation of the 1948 Creeth two-chain model for its structure," *Biochem. Soc. Trans.*, vol. 46, no. 5, pp. 1171–1182, Oct. 2018, doi: 10.1042/BST20180158.

[77] M. Berger, J. A. Gray, and B. L. Roth, "The Expanded Biology of Serotonin," *Annu. Rev. Med.*, vol. 60, no. 1, pp. 355–366, Feb. 2009, doi: 10.1146/annurev.med.60.042307.110802.

[78] J. W. Nelson and R. R. Breaker, "The lost language of the RNA World," *Sci. Signal.*, vol. 10, no. 483, Jun. 2017, doi: 10.1126/scisignal.aam8812.

[79] J. R. Cole *et al.*, "The Ribosomal Database Project: improved alignments and new tools for rRNA analysis," *Nucleic Acids Res.*, vol. 37, no. Database, pp. D141–D145, Jan. 2009, doi: 10.1093/nar/gkn879.

[80] H. M. Salis, "The Ribosome Binding Site Calculator," in *Methods in Enzymology*, vol. 498, Elsevier, 2011, pp. 19–42. doi: 10.1016/B978-0-12-385120-8.00002-4.

[81] J. J. Trausch, P. Ceres, F. E. Reyes, and R. T. Batey, "The Structure of a Tetrahydrofolate-Sensing Riboswitch Reveals Two Ligand Binding Sites in a Single Aptamer," *Structure*, vol. 19, no. 10, pp. 1413–1423, Oct. 2011, doi: 10.1016/j.str.2011.06.019.

[82] A. Peselis and A. Serganov, "Themes and variations in riboswitch structure and function," *Biochim. Biophys. Acta BBA - Gene Regul. Mech.*, vol. 1839, no. 10, pp. 908–918, Oct. 2014, doi: 10.1016/j.bbagrm.2014.02.012.

[83] N. Sudarsan, S. Cohen-Chalamish, S. Nakamura, G. M. Emilsson, and R. R. Breaker, "Thiamine Pyrophosphate Riboswitches Are Targets for the Antimicrobial Compound Pyrithiamine," *Chem. Biol.*, vol. 12, no. 12, pp. 1325–1335, Dec. 2005, doi: 10.1016/j.chembiol.2005.10.007.

[84] M. Media, "Transcription and Translation Regulating Riboswitches. Structure of the Guanine Sensing Riboswitch in its Guanine-Free and -Bound Forms and Comparison with the SAM Riboswitch Type II," *JBSD*. https://www.jbsdonline.com/transcription-and-translation-regulating-riboswitches-structure-guanine-sensing-riboswitch-its-guanine-free-and-bound-forms-and-comparison-sam-riboswitch-type-ii-p15730.html (accessed Dec. 07, 2020).

[85] D. Bhagdikar, F. J. Grundy, and T. M. Henkin, "Transcriptional and translational S-box riboswitches differ in ligand-binding properties," *J. Biol. Chem.*, vol. 295, no. 20, pp. 6849–6860, May 2020, doi: 10.1074/jbc.RA120.012853.

[86] L. Bastet *et al.*, "Translational control and Rho-dependent transcription termination are intimately linked in riboswitch regulation," *Nucleic Acids Res.*, vol. 45, no. 12, pp. 7474–7486, Jul. 2017, doi: 10.1093/nar/gkx434.

[87] K. Strimbu and J. A. Tavel, "What are biomarkers?:," *Curr. Opin. HIV AIDS*, vol. 5, no. 6, pp. 463–466, Nov. 2010, doi: 10.1097/COH.0b013e32833ed177.

[88] Zhuo, Zhenjian, Yuanyuan Yu, Maolin Wang, Jie Li, Zongkang Zhang, Jin Liu, Xiaohao Wu, Aiping Lu, Ge Zhang, and Baoting Zhang. "Recent Advances in SELEX Technology and Aptamer Applications in Biomedicine." *International Journal of Molecular Sciences* 18, no. 10 (2017). https://doi.org/10.3390/ijms18102142.

[89] "Mental health by the numbers," *NAMI*. [Online]. Available: https://www.nami.org/mhstats#:~:text=5.6%25%20of%20U.S.%20adults%20exper

ienced,represents%201%20in%2020%20adults.&text=Annual%20prevalence%20of

%20mental%20illness,Non%2DHispanic%20Asian%3A%2013.9%25. [Accessed: 06-

Jan-2022].

[90] J. N. Zadeh, C. D. Steenberg, J. S. Bois, B. R. Wolfe, M. B. Pierce, A. R. Khan, R. M.

Dirks, N. A. Pierce. NUPACK: analysis and design of nucleic acid systems. *J Comput

Chem*, 32:170–173, 2011.